The Monash Simple Climate Model Experiments (MSCM-DB v1.0): An interactive database of mean climate, climate change and scenario simulations

By Dietmar Dommenget[1*], Kerry Nice[1,4], Tobias Bayr[2], Dieter Kasang[3], Christian Stassen[1] and Mike Rezny[1]

*: corresponding author; dietmar.dommenget@monash.edu
1: Monash University, School of Earth, Atmosphere and Environment, Clayton, Victoria 3800, Australia.
2: GEMOAR Helmholtz Centre for Ocean Research, Düsternbrooker Weg 20, 24105 Kiel, Germany
3: DKRZ, Hamburg, Germany
4: Transport, Health, and Urban Design Hub, Faculty of Architecture, Building, and Planning, University of Melbourne, Victoria 3010, Australia

submitted the Geoscientific Model Development, 8 March 2018

Abstract

This study introduces the Monash Simple Climate Model (MSCM) experiment database. The simulations are based on the Globally Resolved Energy Balance (GREB) model to study three different aspects of climate model simulations: (1) understanding processes that control the mean climate, (2) the response of the climate to a doubling of the CO_2 concentration, and (3) scenarios of external forcing (CO_2 concentration and solar radiation). A series of sensitivity experiments in which elements of the climate system are turned off in various combinations are used to address (1) and (2). This database currently provides more than 1,300 experiments and has an online web interface for fast analysis and free access to the data. We briefly outline the design of all experiments, give a discussion of some results, and put the findings into the context of previously published results from similar experiments. We briefly discuss the quality and limitations of the MSCM experiments and also give an outlook on possible further developments. The GREB model simulation is quite realistic, but does have uncertainties in the mean climate processes in the order of 20-30%. The GREB model without flux corrections has a root mean square error in mean state of the surface temperature of about 10˚C, which is larger than those of general circulation models (2˚C). However, the MSCM experiments show good agreement to previously published studies. Although GREB is a very simple model, it delivers good first-order estimates, is very fast, highly accessible, and can be used to quickly try many different sensitivity experiments or scenarios. It builds

a basis on which conceptual ideas can be tested to a first-order and it provides a null hypothesis for understanding complex climate interactions in the context of response to external forcing or the interactions in the climate subsystems.

1. Introduction

Our understanding of the dynamics of the climate system and climate changes is strongly linked to the analysis of model simulations of the climate system using a range of climate models that vary in complexity and sophistication. Climate model simulations help us to predict future climate changes and they help us to gain a better understanding of the dynamics of this complex system.

State-of-the-art climate models, such as used in the Coupled Model Inter-comparison Project (CMIP; Taylor et al. 2012), are highly complex simulations that require significant amounts of computing resources and time. Such model simulations require a significant amount of preparation. The development of idealized experiments that would help in the understanding and modelling of climate system processes are often difficult to realize with the complex CMIP-type climate models. In this context, simplified climate models are useful, as they provide a fast first guess that help to inform more complex models. They also help in understanding the interactions in the complex system.

In this article, we introduce the Monash Simple Climate Model (MSCM) database (version: MSCM-DB v1.0). The MSCM is an interactive website (http://mscm.dkrz.de, Germany and http://monash.edu/research/simple-climate-model, Australia) and database that provides access to a series of more than 1,300 experiments with the Globally Resolved Energy Balance (GREB) model [Dommenget and Floter 2011; here after referred to as DF11]. The GREB model was primarily developed to conceptually understand the physical processes that control the global warming pattern in response to an increase in CO_2 concentration. It therefore centres around the surface temperature (T_{surf}) tendency equation, and only simulates the processes and variables needed for resolving the global warming pattern.

Simplified climate models, such as Earth System Models of Intermediate Complexity (EMICs), often aim at reducing the complexity to increase the computation speed and therefore allow faster model simulations (e.g. CLIMBER [Petoukhov et al. 2000], UVic [Weaver et al. 2001], FAMOUS [A] or LOVECLIM [Goosse et al. 2010]). These EMICs are very similar in structure to state-of-the-art Coupled General Circulation Models (CGCMs), following the approach of simulating the geophysical fluid dynamics. The GREB model differs, in that it follows an energy balance approach and does not simulate the geophysical fluid dynamics of the atmosphere. It is therefore a climate model that does not include weather dynamics, but focusses on the long term mean climate and its response to external boundary changes.

The purpose of the MSCM database for research studies are the following:

- ***First Guess***: The MSCM provides first guesses for how the climate may change in idealized or realistic experiments. The MSCM experiments can be used to test ideas before implementing and testing them in more detailed CGCM simulations.

- ***Null Hypothesis***: The simplicity of the GREB model provides a good null hypothesis for understanding the climate system. Because it does not simulate weather dynamics or circulation changes of neither large nor small scale it provides the null hypothesis of a climate as a pure energy balance problem.
- ***Conceptual understanding:*** The simplicity of the GREB model helps to better understand the interactions in the complex climate and, therefore, helps to formulate simple conceptual models for climate interactions.
- ***Education***: Studying the results of the MSCM helps to understand the interactions that control the mean state climate and its regional and seasonal differences. It helps to understand how the climate will respond to external forcings in a first-order approximation.

The MSCM provides interfaces for fast analysis of the experiments and selection of the data (see Figs. 1-3). It is designed for teaching and outreach purposes, but also provides a useful tool for researchers. The focus in this study will be on describing the research aspects of the MSCM, whereas the teaching aspects of it will not be discussed. The MSCM experiments focus on three different aspects of climate model simulations: (1) understanding the processes that control the mean climate, (2) the response of the climate to a doubling of the CO_2 concentration, and (3) scenarios of external CO_2 concentration and solar radiation forcings. We will provide a short outline of the design of all experiments, give a brief discussion of some results, and put the findings into context of previously published literature results from similar experiments.
The DF11 study focussed primarily on the development of the model equations and the discussion of the response pattern to an increase in CO_2 concentration. This study here will give a more detailed discussion on the performance of the GREB model on simulation of the mean state climate and on a wider range of external forcing scenarios, including solar radiation changes.
The paper is organized as follows: The following section describes the GREB model, the experiment designs, the MSCM interface, and the input data used. A short analysis of the experiments is given in section 3. This section will mostly focus on the GREB model performance in comparison to observations and previously published simulations in the literature, but it will also give some indications of the findings in the model experiments and the limitations of the GREB model. The final section will give a short summary and outlook for potential future developments and analysis.

2. Model and experiment descriptions

The GREB model is the underlying modelling tool for the MSCM interface. The development of the model and all equations have been presented in DF11. The model is simulating the global climate on a horizontal grid of 3.75° longitude x 3.75° latitude and in three vertical layers: surface, atmosphere and subsurface ocean. It simulates four prognostic variables: surface, atmospheric and subsurface ocean temperature, and atmospheric humidity (column integrated water vapor), see appendix eqs. A1-4. It further simulates a number of diagnostic variables, such as precipitation and snow/ice cover, resulting from the simulation of the prognostic variables.

The main physical processes that control the surface temperature tendencies are simulated: solar (short-wave) and thermal (long-wave) radiation, the hydrological cycle (including evaporation, moisture transport and precipitation), horizontal transport of heat and heat uptake in the subsurface ocean. Atmospheric circulation and cloud cover are seasonally prescribed boundary condition, and state-independent flux corrections are used to keep the GREB model close to the observed mean climate. Thus, the GREB model does not simulate the atmospheric or ocean circulation and is therefore conceptually very different from CGCM simulations.

The model does simulate important climate feedbacks such as the water vapour and ice-albedo feedback, but an important limitation of the GREB model is that the response to external forcings or model parameter perturbations do not involve circulation or cloud feedbacks, which are relevant in CGCM simulations [Bony et al. 2006].

Input climatologies (e.g. T_{surf} or atmospheric humidty) for the GREB model are taken from the NCEP reanalysis data from 1950-2008 [Kalnay et al. 1996], cloud cover climatology from the ISCCP project [Rossow and Schiffer 1991], ocean mixed layer depth climatology from Lorbacher et al. [2006], and topographic data was taken from ECHAM5 atmosphere model [Roeckner et al. 2003].

GREB does not have any internal (natural) variability since daily weather systems are not simulated. Subsequently, the control climate or response to external forcings can be estimated from one single year. The primary advantage of the GREB model in the context of this study is its simplicity, speed, and low computational cost. A one year GREB model simulation can be done on a standard PC computer in about 1 s (about 100,000 simulated years per day). It can do simulations of the global climate much faster than any state-of-the-art climate model and is therefore a good first guess approach to test ideas before they are applied to more complex CGCMs. A further advantage is the lag of internal variability which allows the detection of a response to external forcing much more easily.

a. Experiments for the mean climate deconstruction

The conceptual deconstruction of the GREB model to understand the interactions in the climate system that lead to the mean climate characteristics is done by defining 11 processes (switches; see Fig. 1). For each of these switches, a term in the model equations is set to zero or altered if the switch is "OFF". The processes and how they affect the model equations are briefly listed below (with a short summary in Table 1). The model equations relevant for the experiments in this study are briefly restated in the appendix section A1 for the purpose of explaining each experimental setup in the MSCM.

Ice-albedo: The surface albedo (α_{surf}) and the heat capacity over ocean points (γ_{surf}) are influenced by snow and sea ice cover. In the GREB model these are a direct function of T_{surf}. When the ice-albedo switch is OFF the surface albedo of all points is constant (0.1) and, for ocean points, γ_{surf} follows the prescribed ocean mixed layer depth independent of T_{surf} (i.e. no ice-covered ocean).

Clouds: The cloud cover, CLD, influences the amount of solar radiation reaching the surface (α_{clouds} in eq. [A5]) and the emissivity of the atmospheric layer, ε_{atmos}, for thermal radiation (eq. [A8]). When the clouds switch is OFF, the cloud cover is set to zero.

Oceans: The ocean in the GREB model simulates subsurface heat storage with the surface mixed layer (~upper 50-100m). When the ocean switch is OFF, the F_{ocean} term in eq. [A1] is set to zero, eq. [A3] is set to zero and the heat capacity off all ocean points is set to that of land points.

Atmosphere: The atmosphere in the GREB model simulates a number of processes: The hydrological cycle, horizontal transport of heat, thermal radiation, and sensible heat exchange with the surface. When the atmosphere switch is OFF, eq. [A2] and [A4] are set to zero, the heat flux terms, F_{sense} and F_{latent} in eq. [A1] are set to zero and the downward atmospheric thermal radiation term in eq. [A6] is set to zero.

Diffusion of Heat: The atmosphere transports heat by isotropic diffusion (4th term in eq. [A2]). When this process is switched OFF, the term is set to zero.

Advection of Heat: The atmosphere transports heat by advection following the mean wind field, $\vec{u}$ (5th term in eq. [A2]). When this process is switched OFF, the term is set to zero.

CO_2: The CO_2 concentration affects the emissivity of the atmosphere, ε_{atmos} (eq. [A9]). When this process is switched OFF, the CO_2 concentration is set to zero.

Hydrological cycle: The hydrological cycle in the GREB model simulates the evaporation, precipitation, and transport of atmospheric water vapour (eq. [A4]). It further simulates latent heat cooling at the surface and heating in the atmosphere. When the hydrological cycle is switched OFF, eq. [A4] is set to zero, the heat flux term F_{latent} in eq. [A1] is set to zero, and $viwv_{atmos}$ in eq. [A9] is set to zero. Subsequently, atmospheric humidity is zero.
It needs to be noted here, that the atmospheric emissivity in the log-function parameterization of eq. [A9] can become negative, if the hydrological cycle, cloud cover and CO_2 concentration are switched OFF (set to zero). This marks an unphysical range of the GREB emissivity function and we will discuss the limitations of the GREB model in these experiments in Section 3b.

Diffusion of Water Vapour: The atmosphere transports water vapour by isotropic diffusion (3rd term in eq. [A4]). When this process is switched OFF, the term is set to zero.

Advection of Water Vapour: The atmosphere transports water vapour by advection following the mean wind field, $\vec{u}$ (5th term in eq. [A2]). When this process is switched OFF, the term is set to zero.

Model Corrections: The model correction terms in eqs. [A1, A3 and A4] artificially force the mean T_{surf}, T_{ocean}, and q_{air} climate to be as observed. When

the model correction is switched OFF, the three terms are set to zero. This will allow the GREB model to be studied without any artificial corrections and therefore help to evaluate the GREB model equations' skill in simulating the climate dynamics.

It should be noted here that the model correction terms in the GREB model have been introduced to study the response to doubling of the CO_2 concentration for the current climate, which is a relative small perturbation if compared against the other perturbations considered above. They are meaningful for a small perturbation in the climate system, but are less likely to be meaningful when large perturbations to the climate system are done (e.g. cloud cover set to zero).

Each different combination of the above-mentioned process switches defines a different experiment. However, not all combinations of switches are possible, because some of the process switches are depending on each other (see Table 1 and Fig. 1). The total number of experiments possible with these process switches is 656. For each experiment, the GREB model is run for 50 years, starting from the original GREB model climatology and the final year is presented as the climatology of this experiment in the MSCM database.

b. Experiments for the 2xCO_2 response deconstruction

In a similar way, as described above for the mean climate, the climate response to a doubling of the CO_2 concentration can be conceptually deconstructed with a set of GREB model experiments. These experiments help to understand the interactions in the climate system that lead to the climate response to a doubling of the CO_2 concentration. However, there are a number of differences that need to be considered.

A meaningful deconstruction of the response to a doubling of the CO_2 concentration should consider the reference control mean climate since the forcings and the feedbacks controlling the response are mean state dependent. We therefore ensure that all sensitivity experiments in this discussion have the same reference mean control climate. This is achieved by estimating the flux correction term in eqs. [A1, A3 and A4] for each sensitivity experiment to maintain the observed control climate. Thus, when a process is switched OFF, the control climatological tendencies in eqs. [A1, S3 and S4] are the same as in the original GREB model, but changes in the tendencies due to external forcings, such as doubling of the CO_2 concentration are not affected by the disabled process. This is the same approach as in DF11.

For the 2xCO_2 response deconstruction experiments, we define 10 boundary conditions or processes (switches; see Fig. 2). The Ice-albedo, advection and diffusion of heat and water vapour, and the hydrological cycle processes are defined in the same way as for the mean climate deconstruction (section 2a). The remaining boundary conditions and processes are briefly listed below (and a short summary is given in Table 2).

The following boundary conditions are considered:

Topography: The topography in the GREB model affects the amount of atmosphere above the surface and therefore affects the emissivity of the atmosphere in the thermal radiation (eq. [A9]). Regions with high topography

have less greenhouse gas concentrations in the thermal radiation (eq. [A9]). It further affects the diffusion coefficient (κ) for transport of heat and moisture (eq. [A2 and A4]). When the topography is turned OFF, all points of the GREB model are set to sea level height and have the same amount of CO_2 concentration in the thermal radiation (eq. [A9]).

Clouds: The cloud cover in the GREB model affects the incoming solar radiation and the emissivity of the atmosphere in the thermal radiation (eq. [A9]). In particular, it influences the sensitivity of the emissivity to changes in the CO_2 concentration. A clear sky atmosphere is more sensitive to changes in the CO_2 concentration than a fully cloud-covered atmosphere. When the cloud cover switch is OFF, the observed cloud cover climatology boundary conditions are replaced with a constant global mean cloud cover of 0.7. It is not set to zero to avoid an impact on the global climate sensitivity, and to focus on the regional effects of inhomogeneous cloud cover.

Humidity: Similarly, to the cloud cover, the amount of atmospheric water vapour affects the emissivity of the atmosphere in the thermal radiation and, in particular, the sensitivity to changes in the CO_2 concentration (eq. [A9]). A humid atmosphere is less sensitive to changes in the CO_2 concentration than a dry atmosphere. When the humidity switch is OFF, the constraint to the observed humidity climatology (flux correction in eq. [A4]) is replaced with a constant global mean humidity of 0.0052 [kg/kg]. It is again not set to zero to avoid an impact on the global climate sensitivity, but to focus on the regional effects of inhomogeneous humidity.

The additional feedbacks and processes considered are:

Ocean heat uptake: The ocean heat uptake in GREB is done in two ocean layers. The largest part of the ocean heat is in the subsurface layer, T_{ocean} (eq. [A3]). When the ocean switch is OFF the F_{ocean} term in eq. [A1] is set to zero, equation [A3] is set to zero and the heat capacity (γ_{surf}) off all ocean points in eq. [A1] is set to that of a 50m water column.

The total number of experiments with these process switches is 640. For each experiment, the GREB model is run for 50 years, starting from the original GREB model climatology, and doubling of the CO_2 concentrations in the first time-step. The changes over the 50yrs period relative to the original GREB model climatology of these experiments are presented in the MSCM database.

c. Scenario experiments

A number of different scenarios of external boundary condition changes exist in the MSCM experiment database. They include different changes in the CO_2 concentration and in the incoming solar radiation. A complete overview is given in Table 3. A short description follows below.

RCP-scenarios

In the Representative Concentration Pathways (RCP) scenarios the GREB model is forced with time varying CO_2 concentrations. All five different simulations have

the same historical time evolution of CO_2 concentrations starting from 1850 to 2000, and from 2001 follow the RCP8.5, RCP6, RCP4.5, RCP2.6 and the A1B CO_2 concentration pathways until 2100 [van Vuuren et al. 2011].

Idealized CO_2 scenarios

The 15 idealized CO_2 concentration scenarios in the MSCM experiment database focus on the non-linear time delay and regional differences in the climate response to different CO_2 concentrations. These were implemented in five simulations in which the control CO_2 concentration (340ppm) was changed in the first time step to a scaled CO_2 concentration of 0, 0.5, 2, 4, and 10 times the control level. The 0.5xCO_2 and 2xCO_2 simulations are 50yrs long and the others are 100yrs long.

Two different simulations with idealized time evolutions of CO_2 concentrations are conducted to study the time delay of the climate response. In one simulation, the CO_2 concentration is doubled in the first time-step, held at this level for 30yrs then returned to control levels instantaneously (2xCO_2 abrupt reverse). In the second simulation, the CO_2 concentration is varied between the control and 2xCO_2 concentrations following a sine function with a period of 30yrs, starting at the minimum of the sine function at the control CO_2 concentration (2xCO_2 wave). Both simulations are 100yrs long.

The third set of idealized CO_2 concentration scenarios double the CO_2 concentrations restricted to different regions or seasons. The eight regions and seasons include: the Northern or Southern Hemisphere, tropics (30°S-30°N) or extra-tropics (poleward of 30°), land or oceans and in the month October to March or in the month April to September. Each experiment is 50yrs long.

Solar radiation

Two different experiments with changes in the solar constant were created. In the first experiment, the solar constant is increased by about 2% (+27W/m^2), which leads to about the same global warming as a doubling of the CO_2 concentration [Hansen et al. 1997]. In the second experiment, the solar constant oscillates at an amplitude of 1W/m^2 and a period of 11yrs, representing an idealized variation of the incoming solar short wave radiation due to the natural 11yr solar cycle [Willson and Hudson 1991]. Both experiments are 50yrs long.

Idealized orbital parameters

A series of five simulations are done in the context of orbital forcings and the related ice age cycles. In one simulation, the incoming solar radiation as function of latitude and day of the year was changed to its values as it was 231Kyrs ago [Berger and Loutre 1991 and Huybers 2006]. In an additional simulation, the CO_2 concentration is reduced from 340ppm to 200ppm as observed during the peak of ice age phases in combination with the incoming solar radiation changes. Both simulations are 100yrs long.

In three sensitivity experiments, we changed the incoming solar radiation according to some idealized orbital parameter changes to study the effect of the most important orbital parameters. The orbital parameters changed are: the distance to the sun, the Earth axis tilt relative to the Earth-Sun plane (obliquity) and the eccentricity of the Earth orbit around the sun. The orbit radius was changed from 0.8AU to 1.2AU in steps of 0.01AU, the obliquity from -25° to 90° in

steps of 2.5° and the eccentricity from 0.3 (Earth closest to the sun in July) to 0.3 (Earth furthest from the sun in July) in steps of 0.01. Each sensitivity experiment was started from the control GREB model (1AU radius, 23.5° obliquity and 0.017 eccentricity) and run for 50yrs. The last year of each simulation is presented as the estimate for the equilibrium climate.

3. Some results of the model simulations

The MSCM experiment database includes a large set of experiments that address many different aspects of the climate. At the same time, the GREB model has limited complexity and not all aspects of the climate system are simulated in the GREB experiments. The following analysis will give a short overview of some of the results that can be taken from the MSCM experiments. In this we will focus on aspects of general interest and on comparing the outcome to results of other published studies to illustrate the strength and limitations of the GREB model in this context. The discussion, however, will be incomplete, as there are simply too many aspects that could be discussed in this set of experiments. We will therefore focus on a general introduction and leave space for future studies to address other aspects.

a. GREB model performance

The skill of the GREB model is illustrated in Figure 4, by running the GREB model without the correction terms. For reference, we compare this GREB run with the observed mean climate and seasonal cycle (this is identical to running the GREB model with correction terms) and with a bare world. The latter is the GREB model with all switches OFF (radiative balance without an atmosphere and a dark surface). In comparison with the full GREB model, this illustrates how much all the climate processes affect the climate.

The GREB model without correction terms does capture the main features of the zonal mean climate, the seasonal cycle, the land-sea contrast and even smaller scale structures within continents or ocean basins (e.g. seasonal cycle structure within Asia or zonal temperature gradients within ocean basins). For most of the globe (<50° from the equator), the GREB model root-mean-squared error (RMSE) for the annual mean T_{surf} is less than 10°C relative to the observed (see Fig. 4g). This is larger than for state-of-the-art CMIP-type climate models, which typically have an RMSE of about 2°C [Dommenget 2012]. In particular, the regions near the poles have high RMSE. It seems likely that the meridional heat transport is the main limitation in the GREB model, given the too warm tropical regions and the, in general, too cold polar regions and the too strong seasonal cycle in the polar regions in the GREB model without correction terms.

The GREB model performance can be put in perspective by illustrating how much the climate processes simulated in the GREB model contribute to the mean climate relative to the bare world simulation (see Fig. 4). The GREB RMSE to observed is about 20-30% of the RMSE of the bare world simulation (not shown), suggesting that the GREB model has a relative error of about 20-30% in the processes that it simulates or due to processes that it does not simulate (e.g. ocean heat transport).

b. Mean climate deconstruction

Understanding what is causing the mean observed climate with its regional and seasonal difference is often central for understanding climate variability and change. For instance, the seasonal cycle is often considered as a first guess estimate for climate sensitivity [Knutti et al. 2006]. In the following analysis, we will give a short overview on how the 10 processes of the MSCM experiments contribute to the mean climate and its seasonal cycle. For these experiments, we use the GREB model without flux correction terms.

In the discussion of the experiments, it is important to consider that climate feedbacks are contributing to the interactions of the climate processes. The effect of a climate process on the climate is a result of all the other active climate processes responding to the changes that the climate process under consideration introduces. It also depends on the mean background climate. Therefore, it does matter in which combination of switches the GREB model experiments are discussed. For instance, the effect of the Ice/Snow cover, is stronger in a much colder background climate, but is also affected by the feedback in other climate processes, such as the water vapour feedback. We will therefore consider different experiments or different experiment sets to shade some light into these interactions.

In Figures 5 and 6 the contribution of each of the 10 processes (except the atmosphere) to the annual mean climate (Fig. 5) and its seasonal cycle (Fig. 6) are shown. In each experiment, all processes are active, but the process of interest and the model correction terms are turned OFF. The results are compared against the complete GREB model without the model correction terms (all processes active; expect model correction terms). For the hydrological we will discuss some additional experiments in which the ice-albedo feedback is turned OFF as well.

The Ice/Snow cover (Fig. 5a) has a strong cooling effect mostly at the high latitudes in the cold season, which is due to the ice-albedo feedback. However, in the warm season (not shown) the insulation effect of the sea ice actually leads to warming, as the ocean cannot cool down as much during winter as it does without sea ice.

The cloud cover in the GREB model is only considered as a given boundary condition, but does not simulate the formation of clouds. Therefore, it does not include cloud feedbacks. However, the mean cloud cover does influence the radiation balance and therefore affects the mean climate and its seasonal cycle. Fig. 5b illustrates that cloud cover has a large net cooling effect globally due to the solar radiation reflection effect dominating over the thermal radiation warming effect. Previous studies on the cloud cover effect on the overall climate mostly focus on the radiative forcings estimates, but to our best knowledge do not present the overall change in surface temperature [e.g. Rossow and Zhang 1995].

It is interesting to note that the strongest cooling effect of cloud cover is over regions with fairly little cloud cover (e.g. deserts and mountain regions). Here it is important to point out that the climate system response to any external forcing or changes in the boundary conditions, such as CO_2-forcing or removing the cloud cover, is dominated by internal positive feedback rather than the direct local forcing effect (e.g. see discussion of the global warming pattern in DF11).

The most important internal positive feedback is the water vapor feedback, which amplifies the effect of removing the cloud cover. This feedback is stronger over dry and cold regions (DF11) and therefore amplifies the effects of removing the cloud cover over deserts and mountain regions.

The large ocean heat capacity slows down the seasonal cycle (Fig. 6c). Subsequently, the seasons are more moderate than they would be without the ocean transferring heat from warm to cold seasons. This is, in particular, important in the mid and higher latitudes. The effect of the ocean heat capacity, however, has also an annual mean warming effect (Fig. 5c). This is due to the non-linear thermal radiation cooling. The non-linear black body negative radiation feedback is stronger for warmer temperatures, which are not reached in a moderated seasonal cycle with the larger ocean heat capacity. Studies with more complex climate models do fine similar impacts of the ocean heat capacity on the annual mean and on the seasonal cycle (e.g. Donohoe et al. 2014).

The diffusion of heat reduces temperature extremes (Fig. 5d). It therefore warms extremely cold regions (e.g. polar regions) and cools the hottest regions (e.g. warm deserts). In global averages, this is mostly cancelled out. The advection of heat has strong effects where the mean winds blow across strong temperature gradients. This is mostly present in the Northern Hemisphere (Fig. 5e). The most prominent feature is the strong warming of the northern European and Asian continents in the cold season. In global average, warming and cooling mostly cancel each other out.

Literature discussions of heat transport are usually based on heat budget analysis of the climate system (in observations or simulations) instead 'switching off' the heat transport in fully complex climate models, since such experiments are difficult to conduct. A similar heat budget analysis of the GREB model experiments is beyond the scope of this study, but the results in these experiments appear to be largely consistent with the findings in heat budget analysis. For instance, the regional contributions of diffusion and advection are similar to those found in previous studies (e.g. Peixoto 1992; Yang et al. 2015).

The CO_2 concentration leads to a global mean warming of about 9 degrees (Fig. 5f). Even though it is the same CO_2 concentration everywhere, the warming effect is different at different locations. This is discussed in more detail in DF11 and in section 3c.

The input of water vapour into the atmosphere by the hydrological cycle leads to a substantial amount of warming globally (Fig. 5g). However, we need to consider that the experiment with switching OFF the hydrological cycle is the only experiment in which we have a significant amount of global cooling (by about -44˚C). As a result, most of the earth is below freezing temperatures and therefore has a much stronger ice-albedo feedback than in any other experiment. This leads to a significant amplification of the response.

It is instructive to repeat the experiments with the ice-albedo feedback switched OFF (see supplementary Fig. 1). In these experiments, all processes show a reduced impact on the annual mean temperatures, but the hydrological cycle is most strongly affected by it. The ice-albedo effect almost doubles the hydrological cycle response, while for all other processes the effect is about a 10% to 40% increase. In the following discussions, we will therefore consider the hydrological cycle impact with and without ice-albedo feedback. In the average of both response (Fig. 5g and SFig. 1g) the hydrological cycle has a global

mean impact of about +34˚C with strongest amplitudes in the tropics. It is still the strongest of all processes.

Similar to the oceans, the hydrological cycle dampens the seasonal cycle (Fig. 6g), but with a much weaker amplitude. The transport of water vapour away from warm and moist regions (e.g. tropical oceans) to cold and dry regions (e.g. high latitudes and continents) leads to additional warming in the regions that gain water vapour and cooling to those that lose water vapour (Fig. 6h). The effect is similar in both hemispheres. The transport of water vapour along the mean wind directions has stronger effects on the Northern Hemisphere than on the Southern Hemisphere, since the northern hemispheric mean winds have more of a meridional component, which creates advection across water vapour gradients (Fig. 6i). This effect is most pronounced in the cold seasons.

Most processes have a predominately zonal structure. We can therefore take a closer look at the zonal mean climate and seasonal cycle of all processes to get a good representation of the relative importance of each process, see Fig. 7. The annual mean climate is most strongly influenced by the hydrological cycle (here shown as the mean of the response with and without the ice-albedo feedback). The cloud cover has an opposing cooling effect, but is weaker than the warming effect of the hydrological cycle. The warming effect by the ocean's heat capacity is similar in scale to that of the CO_2 concentration.

An interesting aspect of the climate system is that the Northern hemisphere is warmer than the Southern counterpart (by about 1.5^{o}C; not shown), which may be counterintuitive given the warming effect of the ocean heat capacity (see above discussion; Kang et al. 2015). The GREB model without flux correction also does have a warmer Northern hemisphere than the Southern counterpart (by about 0.3^{o}C; not shown), whereas the bare earth (pure blackbody radiation balance; GREB all switches OFF) would have the Northern hemisphere colder than the Southern counterpart (by about -0.6^{o}C; not shown). A number of processes play into this inter-hemispheric contrast, with the most important contribution coming from the cross-equatorial heat and moisture advection (see Fig. 7a). This is largely consistent with Kang et al. (2015).

The seasonal cycle is damped most strongly by the ocean's heat capacity and by the hydrological cycle. The latter may seem unexpected, but is due to the effect that the increased water vapour has a stronger warming effect in the cold seasons, similarly to the greenhouse effect of CO_2 concentrations. In turn, the ice/snow cover and cloud cover lead to an intensification of the seasonal cycle at higher latitudes. Again, the latter may seem unexpected, but is due to the interaction with other climate feedbacks such as the water vapour feedback, which also makes the climate more strongly respond to changes in cloud cover in regions where there actually is very little cloud cover (e.g. deserts).

As an alternative way of understanding the role of the different process we can build up the complete climate by introducing one process after the other, see Figs. 8 and 9. We start with the bare earth (e.g. like our Moon) and then introduce one process after the other. The order in which the processes are introduced is mostly motivated by giving a good representation for each of the 10 processes. However, it can also be interpreted as a build up the Earth climate in a somewhat historical way: We assume that initially the earth was a bare planet and then the atmosphere, ocean, and all the other aspects were build up over time.

The Bare Earth (all switches OFF) is a planet without atmosphere, ocean or ice. It has an extremely strong seasonal cycle (Fig. 9a) and is much colder than our current climate (Fig. 8a). It also has no regional structure other than meridional temperature gradients. The combination of all climate processes will create most of the regional and seasonal difference that make our current climate.

The atmospheric layer in the GREB model simulates two processes, if all other processes are turned off: a turbulent sensible heat exchange with the surface and thermal radiation due to residual trace gasses other than CO_2, water vapour or clouds. However, as mentioned in the appendix A1 the log-function approximation leads to negative emissivity if all greenhouse gasses (CO_2 and water vapour) concentrations and cloud cover are zero. The negative emissivity turns the atmospheric layer into a cooling effect, which dominates the impact of the atmosphere in this experiment (Figs. 8b, c). This is a limitation of the GREB model and the result of this experiment as such should be considered with caution. In a more realistic experiment we can set the emissivity of the atmosphere to zero or a very small value (0.01) to simulate the effect of the atmosphere without CO_2, water vapour and cloud cover, see SFig. 2. Both experiments have very similar warming effects in polar regions. Suggesting that the sensible heat exchange warms the surface. The residual thermal radiation effect from the emissivity of 0.01 has only a minor impact (SFig. 2f and g).

The warming effect of the CO_2 concentration is nearly uniform (Figs. 8d, e) and without much of a seasonal cycle (Figs. 9d, e), if all other processes are turned OFF. This accounts for a warming of about +9˚C.

The oceans reduce the seasonal cycle by their large heat capacity (Figs. 9f, g). The effective heat capacity of the oceans is proportional to the observed mixed layer in the GREB model, which causes some small variations (differences from the zonal means) as seen in the seasonal cycle of the oceans. Land points are not affected, since no atmospheric transport exist (advection and diffusion turned OFF). The different heat capacity between oceans and land already make a significant element of the regional and seasonal climate differences (Figs. 8f, g).

Introducing turbulent diffusion of heat in the atmosphere now enables interaction between points, which has the strongest effects along coastlines and in higher latitudes (Figs. 8h, i). It reduces the land-sea contrast and has strong effects over land with warming in winter and cooling in summer (Figs. 9h, i). The extreme climates of the winter polar region are most strongly affected by the turbulent heat exchange with lower latitudes. The turbulent heat exchange makes the regional climate difference again a bit more realistic.

The advection of heat is strongly dependent on the temperature gradients along the mean wind field directions. It provides substantial heating during the winter season for Europe, Russia, and western North America (Figs. 8j, k, 9j, k). The structure (differences from the zonal mean) created by this process is mostly caused by the prescribed mean wind climatology. In particular, the milder climate in Europe compared to northeast Asia on the same latitudes, are created by wind blowing from the ocean onto land. The same is true for the differences between the west and east coasts of northern North America. The climate regional and seasonal structures are now already quite realistic, but the overall climate is much too cold. The ice/snow cover further cools the climate, in particular, the polar regions (Figs. 8l, m). This difference illustrates that the ice-

albedo feedback is primarily leading to cooling in higher latitudes and mostly in the winter season.

Introducing the hydrological cycle brings the most important greenhouse gas into the atmosphere: water vapour. This has an enormous warming effect globally (Figs. 8n, o) and a moderate reduction in the strength of the seasonal cycle (Figs. 9n, o). The resulting modelled climate is now much too warm, but introducing the cloud cover cools the climate substantially (Figs. 8p, q) and leads to a fairly realistic climate.

The atmospheric transport (diffusion and advection) brings water vapour from relative moist regions to relatively dry regions (Figs. 8r, s). This leads to enhanced warming in the dry and cold regions (e.g. Sahara Desert or polar regions) by the water vapour thermal radiation (greenhouse) effect and cooling in the regions where it came from (e.g. tropical oceans). The heating effect is similar to the transport of heat and has also a strong seasonal cycle component.

c. 2xCO_2 response deconstruction

The doubling of the CO_2 concentrations leads to a distinct warming pattern with polar amplification, a land-sea contrast and significant seasonal differences in the warming rate. These structures in the warming pattern reflect the complex interactions between feedbacks in the climate system and regional difference in CO_2 forcing pattern. The MSCM 2xCO_2 response experiments are designed to help understand the interactions causing this distinct warming pattern. DF11 discussed many aspects of these experiments with focus on the land-sea contrast, the seasonal differences, and the polar amplification. We therefore will focus here only on some aspects that have not been previously discussed in DF11.

In the GREB model, we can turn OFF the atmospheric transport and therefore study the local interaction without any lateral interactions. Figure 10 shows three experiments in which the atmospheric transport and other processes (see Figure caption) are inactive. The three experiments highlight the regional difference in the CO_2 forcing pattern and in the two main feedbacks (water vapour and ice-albedo).

In the first experiment (Fig. 10a) without feedback processes, the local T_{surf} response is approximately directly proportional to the local CO_2 forcing. The regional differences are caused by differences in the cloud cover and atmospheric humidity, since both influence the thermal radiation effect of CO_2 [DF11, Kiehl and Ramanathan 1982 and Cess et al. 1993]. This causes, on average, the land regions to see a stronger forcing than oceanic regions (see Fig. 10b). However, even over oceans we can see clear differences. For instance, the warm pool of the western tropical Pacific sees less CO_2 forcing than the eastern tropical Pacific.

The ice-albedo feedback is strongly localized and it is strongest over the mid-latitudes of the northern continents and at the sea ice edge of around Antarctica (Figs. 10c and d). The water vapour feedback is far more wide-spread and stronger (Figs. 10e and f). It is strongest in relatively warm and dry regions (e.g. subtropical oceans), but also shows some clear localized features, such as the strong Arabian or Mediterranean Seas warming.

d. Scenarios

The set of scenario experiments in the MSCM simulations allows us to study the response of the climate system to changes in the external boundary conditions in a number of different ways. In the following, we will briefly illustrate some results from these scenarios and organize the discussion by the different themes in scenario experiments.

The CMIP project has defined a number of standard CO_2 concentration projection simulations, that give different RCP scenarios for the future climate change, see Fig. 11a. The GREB model sensitivity in these scenarios is similar to those of the CMIP database [Forster et al. 2013].

Idealized CO_2 concentration scenarios help to understand the response to the CO_2 forcing. In Figure 11b, we show the global mean T_{surf} response to different scaling factors of CO_2 concentrations. To first order, we can see that the global mean T_{surf} response follows a logarithmic CO_2 concentration (e.g. any doubling of the CO_2 concentration leads to the same global mean T_{surf} response; compare 2xCO_2 with 4xCO_2 or with in Fig.11b) as suggested in other studies [Myhre et al. 1998]. However, this relationship does breakdown if we go to very low CO_2 concentrations (e.g. zero CO_2 concentration) illustrating that the log-function approximation of the CO_2 forcing effect is only valid within a narrow range far away from zero CO_2 concentration.

The transient response time to CO_2 forcing can be estimated from idealized CO_2 concentration changes, see Fig. 11c. The step-wise change in CO_2 concentration illustrates the response time of the global climate. In the GREB model, it takes about 10yrs to get 80% of the response to a CO_2 concentration change (see step-function response, Fig. 11c). In turn, the response to a CO_2 concentration wave time evolution is a lag of about 3yrs. The fast versus slow response also leads to different warming patterns with strong land-sea contrasts (not shown), that are largely similar to those found in previous studies [Held et al. 2010].

The regional aspects of the response to a CO_2 concentration can also be studied by partially increasing the CO_2 concentration in different regions, see Fig. 12. The warming response mostly follows the regions where we partially changed the CO_2 concentration, but there are some interesting variations in this. The partial increase in the CO_2 concentration over oceans has a stronger warming impact than the partial increase in the CO_2 concentration over land for most Southern Hemisphere land regions. In turn, the land forcing has little impact for the ocean regions. The boreal winter forcing has stronger impact on the Southern Hemisphere than boreal summer forcing, suggesting that the warm season forcing is, in general, more important than the cold season forcing. The only exception to this is the Tibet-plateau region.

A series of scenarios focus on the impact of solar forcing. In Figure 11d, we show the response to an idealized 11yr solar cycle. The global mean T_{surf} response is two orders of magnitude smaller than the response to a doubling of the CO_2 concentration, reflecting the weak amplitude of this forcing. This result is largely consistent with the response found in GCM simulations [Cubasch et al. 1997], but does not consider possible more complicated amplification mechanisms [Meehl et al. 2009]. A change in the solar constant of +27W/m^2 has a global T_{surf} warming response similar to a doubling of the CO_2 concentration, but with a slightly different warming pattern, see Fig. 13. The warming pattern of a solar constant change has a stronger warming where incoming sun light is stronger

(e.g. tropics or summer season) and a weaker warming in region with less incoming sun light (e.g. higher latitudes or winter season). This is in general agreement with other modelling studies [Hansen et al. 1997].

On longer paleo time scales (>10,000yrs), changes in the orbital parameters affect the incoming sun light. Figure 14 illustrates the response to a number of orbital solar radiation changes. Incoming radiation (sunlight) typical of the ice age (231kyrs ago) has less incoming sunlight in the Northern Hemispheric summer. However, it has every little annual global mean changes (Fig. 14a) due to increases in sunlight over other regions and seasons. The T_{surf} response pattern in the zonal mean at the different seasons is very similar to the solar forcing, but the response is slightly more zonal and seasonal differences are less dominant (Fig. 14b). The response is also amplified at higher latitudes. However, in the global mean there is no significant global cooling as observed during ice ages. If the solar forcing is combined with a reduction in the CO_2 concentration (from 340ppm to 200ppm), we find a global mean cooling of -1.7°C (Fig. 14c), which is still much weaker than observed during ice ages, but is largely consistent with previous studies of simulations of ice age conditions [Weaver et al. 1998, Braconnot et al. 2007]. This is not unexpected since the GREB model does not include an ice sheet model and, therefore, does not include glacier growth feedbacks that would amplify ice age cycles.

A better understanding of the orbital solar radiation forcing can be gained by analysing the response to idealized orbital parameter changes. We therefore vary the Earth distance to the sun (radius), the earth axis tilt to the earth orbit plane (obliquity) and shape of the earth orbit around the sun (eccentricity) over a wider range, see Figs. 14 d-f. When the radius is changed by 10%, the Earth climate becomes essentially uninhabitable, with either global mean temperature above 30°C (approx. summer mean temperature of the Sahara) or a completely ice-covered snowball Earth. This suggests that the habitable zone of the Earth radius is fairly small due to the positive feedbacks within the climate system simulated in the GREB model (not considering long-term or more complex atmospheric chemistry feedbacks) and largely consistent with previous studies [Kasting et al. 1993].

When the obliquity is zero, the tropics become warmer and the polar regions cool down further than today's climate, as they now receive very little sunlight throughout the whole year. In the extreme case, when the obliquity is 90°, the tropics become ice covered and cooler than the polar regions, which are now warmer than the tropics today and ice free. The polar regions now have an extreme seasonal cycle (not shown), with sunlight all day during summer and no sunlight during winter. Any eccentricity increase in amplitude would lead to a warmer overall climate. Thus, a perfect circle orbit around the sun has, on average, the coldest climate and all of the more extreme eccentricity (elliptic) orbits have warmer climates. This suggests that the warming effect of the section of the orbit that has a closer transit around the sun in an eccentricity orbit relative to the perfect circle orbit overcompensates the cooling effect of the more remote transit around the sun in the other half of the orbit relative to the perfect circle orbit.

4. Summary and discussion

In this study, we introduced the MSCM database (version: MSCM-DB v1.0) for research analysis with more than 1,300 experiments. It is based on model simulations with the GREB model for studies of the processes that contribute to the mean climate, the response to doubling of the CO_2 concentration, and different scenarios with CO_2 or solar radiation forcings. The GREB model is a simple climate model that does not simulate internal weather variability, circulation, or cloud cover changes. It provides a simple and fast null hypothesis for the interactions in the climate system and its response to external forcings.

The GREB model without flux corrections simulates the mean observed climate well and has an uncertainty of about 10˚C. The model has larger cold biases in the polar regions indicating that the meridional heat transport is not strong enough. Relative to a bare world without any climate processes the RMSE is reduced to about 20-30% relative to observed. Thus, as a first guess, it can be assumed that the GREB model simulations gives a 20-30% uncertainty in the processes it simulates. Further, the GREB models emissivity function reaches unphysical negative values when water vapour, CO_2 and cloud cover is set to zero. This is a limitation of the log-function parametrization, that can potentially be revised if a new parameterization is developed that considers these cases. However, it is beyond the scope of this study to develop such a new parameterization and it is left for future studies.

The MSCM experiments for the conceptual deconstruction of the observed mean climate provide a good understanding of the processes that control the annual mean climate and its seasonal cycle. The cloud cover, atmospheric water vapour, and the ocean heat capacity are the most important processes that determine the regional difference in the annual mean climate and its seasonal cycle. The observed seasonal cycle is strongly damped not only by the ocean heat capacity, but also by the water vapour feedback. In turn, ice-albedo and cloud cover amplify the seasonal cycle in higher latitudes.

The conceptual deconstruction of the response to a doubling of the CO_2 concentration based on the MSCM experiments has mostly been discussed in DF11, but some additional results shown here focused on the local forcing in response without horizontal interaction. It has been shown here that the CO_2 forcing has a clear land-sea contrast, supporting the land-sea contrast in the T_{surf} response. The water vapour feedback is wide-spread and most dominant over the subtropical oceans, whereas the ice-albedo feedback is more localized over Northern Hemispheric continents and around the sea ice border.

The series of scenario simulations with CO_2 and solar forcing provide many useful experiments to understand different aspects of the climate response. The RCP and idealized CO_2 forcing scenarios give good insights into the climate sensitivity, regional differences, transient effects, and the role of CO_2 forcing at different seasons or locations. The solar forcing experiments illustrate the subtle differences in the warming pattern to CO_2 forcing and the orbital solar forcing experiments illustrated elements of the climate response to long term, paleo, climate forcings.

In summary, the MSCM provides a wide range of experiments for understanding the climate system and its response to external forcings. It builds a basis on which conceptual ideas can be tested to a first-order and it provides a null hypothesis for understanding complex climate interactions. Some of the

experiments presented here are similar to previously published simulations. In general, the GREB model results agree well with the results of more complex GCM simulations. It is beyond the scope of this study to discuss all aspects of the experiments and their results. This will be left to future studies. Here we need to keep in mind the limitation that the GREB model does not consider atmospheric or ocean circulation changes nor does it simulate cloud cover feedbacks. Such processes will alter this picture somewhat and need to be studied with more complex climate models, which may in particular be important for more detailed regional information of future climate change or social-economical impact studies.

Future development of this MSCM database will continue and it is expected that this database will grow. The development will go in several directions: the GREB model performance in the processes that it currently simulates will be further improved. In particular, the simulation of the hydrological cycle needs to be improved to allow the use of the GREB model to study changes in precipitation. Simulations of aspects of the large-scale atmospheric circulation, aerosols, carbon cycle, or glaciers would further enhance the GREB model and would provide a wider range of experiments to run for the MSCM database.

5. Code and data availability

The MSCM model code, including all required input files, to do all experiments described on the MSCM homepage and in this paper, can be downloaded as compressed tar archive from the MSCM homepage under

http://mscm.dkrz.de/download/mscm-web-code.tar.gz

or from the bitbucket repository under

https://bitbucket.org/tobiasbayr/mscm-web-code

The data for all the experiments of the MSCM can be accessed via the MSCM webpage interface (DOI: 10.4225/03/5a8cadac8db60). The mean deconstruction experiments file names have an 11 digits binary code that describe the 11 process switches combination: 1=ON and 0=OFF. The digit from left to right present the following processes:

1. Model corrections
2. Ice albedo
3. Cloud cover
4. Advection of water vapour
5. Diffusion of water vapour
6. Hydrologic cycle
7. Ocean
8. CO_2
9. Advection of heat
10. Diffusion of heat
11. Atmosphere

For example, the data file *greb.mean.decon.exp-10111111111.gad* is the experiment with all processes ON, but ice albedo is OFF. The 2x CO_2 response deconstruction experiments file names have a 10 digits binary code that describe the 10 process switches combination. The digit from left to right present the following processes:

1. Ocean heat uptake
2. Advection of water vapour
3. Diffusion of water vapour
4. Hydrologic cycle
5. ice albedo
6. Advection of heat
7. Diffusion of heat
8. Humidity (climatology)
9. Clouds (climatology)
10. Topography (Observed)

For example, the data file *response.exp-0111111111.2xCO2.gad* is the experiment with all processes ON, but ocean heat uptake is OFF. The individual experiments can be chosen from the webpage interface by selecting the desired switch combinations. Alternatively, all experiments can be downloaded in a combined tar-file from the webpage interface.
For all experiments, the datasets includes five variables: surface, atmospheric and subsurface ocean temperature, atmospheric humidity (column integrated water vapor) and snow/ice cover.

Acknowledgments

This study was supported by the ARC Centre of Excellence for Climate System Science, Australian Research Council (grant CE110001028). The development of the MSCM webpages was support by a number of groups (see MSCM webpages). Special thanks go to Martin Schweitzer for his work on the first prototype of the MSCM webpages.

References

Berger, A., and M. F. Loutre, 1991: Insolation Values for the Climate of the Last 10000000 Years. *Quaternary Sci Rev*, **10,** 297-317.

Bony, S., and Coauthors, 2006: How well do we understand and evaluate climate change feedback processes? *Journal of Climate*, **19,** 3445-3482.

Braconnot, P., and Coauthors, 2007: Results of PMIP2 coupled simulations of the Mid-Holocene and Last Glacial Maximum - Part 1: experiments and large-scale features. *Clim Past*, **3,** 261-277.

Cess, R. D., and Coauthors, 1993: Uncertainties in Carbon-Dioxide Radiative Forcing in Atmospheric General-Circulation Models. *Science*, **262,** 1252-1255.

Cubasch, U., R. Voss, G. C. Hegerl, J. Waszkewitz, and T. J. Crowley, 1997: Simulation of the influence of solar radiation variations on the global climate with an ocean-atmosphere general circulation model. *Climate Dynamics*, **13,** 757-767.

Donohoe, A., D. M. W. Frierson, and D. S. Battisti, 2014: The effect of ocean mixed layer depth on climate in slab ocean aquaplanet experiments. *Clim. Dyn.*, **43**, 1041–1055, doi:10.1007/s00382-013-1843-4.

Dommenget, D., 2012: Analysis of the Model Climate Sensitivity Spread Forced by Mean Sea Surface Temperature Biases. *Journal of Climate*, **25,** 7147-7162.

Dommenget, D., and J. Floter, 2011: Conceptual understanding of climate change with a globally resolved energy balance model. *Climate Dynamics*, **37,** 2143-2165.

Forster, P. M., T. Andrews, P. Good, J. M. Gregory, L. S. Jackson, and M. Zelinka, 2013: Evaluating adjusted forcing and model spread for historical and future scenarios in the CMIP5 generation of climate models. *Journal of Geophysical Research-Atmospheres*, **118,** 1139-1150.

Goosse, H., and Coauthors, 2010: Description of the Earth system model of intermediate complexity LOVECLIM version 1.2. *Geosci Model Dev*, **3,** 603-633.

Hansen, J., M. Sato, and R. Ruedy, 1997: Radiative forcing and climate response. *Journal of Geophysical Research-Atmospheres*, **102,** 6831-6864.

Held, I. M., M. Winton, K. Takahashi, T. Delworth, F. R. Zeng, and G. K. Vallis, 2010: Probing the Fast and Slow Components of Global Warming by Returning Abruptly to Preindustrial Forcing. *Journal of Climate*, **23,** 2418-2427.

Huybers, P., 2006: Early Pleistocene glacial cycles and the integrated summer insolation forcing. *Science*, **313,** 508-511.

Kalnay, E., and Coauthors, 1996: The NCEP/NCAR 40-year reanalysis project. *Bulletin of the American Meteorological Society*, **77,** 437-471.

Kang, S. M., R. Seager, D. M. W. Frierson, and X. Liu, 2015: Croll revisited: Why is the northern hemisphere warmer than the southern hemisphere? *Clim. Dyn.*, **44**, 1457–1472, doi:10.1007/s00382-014-2147-z.

Kasting, J. F., D. P. Whitmire, and R. T. Reynolds, 1993: Habitable Zones around Main-Sequence Stars. *Icarus*, **101,** 108-128.

Kiehl, J. T., and V. Ramanathan, 1982: Radiative Heating Due to Increased Co2 - the Role of H2o Continuum Absorption in the 12-18 Mu-M Region. *Journal of the Atmospheric Sciences*, **39,** 2923-2926.

930 Knutti, R., G. A. Meehl, M. R. Allen, and D. A. Stainforth, 2006: Constraining
931 climate sensitivity from the seasonal cycle in surface temperature. *Journal*
932 *of Climate*, **19,** 4224-4233.
933 Lorbacher, K., D. Dommenget, P. P. Niiler, and A. Kohl, 2006: Ocean mixed layer
934 depth: A subsurface proxy of ocean-atmosphere variability. *Journal of*
935 *Geophysical Research-Oceans*, **111,** -.
936 Meehl, G. A., J. M. Arblaster, K. Matthes, F. Sassi, and H. van Loon, 2009:
937 Amplifying the Pacific Climate System Response to a Small 11-Year Solar
938 Cycle Forcing. *Science*, **325,** 1114-1118.
939 Myhre, G., E. J. Highwood, K. P. Shine, and F. Stordal, 1998: New estimates of
940 radiative forcing due to well mixed greenhouse gases. *Geophysical*
941 *Research Letters*, **25,** 2715-2718.
942 Peixoto, J. P. and A. H. O., 1992: *Physics of Climate*. Springer US,.
943 Petoukhov, V., A. Ganopolski, V. Brovkin, M. Claussen, A. Eliseev, C. Kubatzki, and
944 S. Rahmstorf, 2000: CLIMBER-2: a climate system model of intermediate
945 complexity. Part I: model description and performance for present
946 climate. *Climate Dynamics*, **16,** 1-17.
947 Roeckner, E., and Coauthors, 2003: The atmospheric general circulation model
948 ECHAM 5. Part I: Model description. *Reports of the Max-Planck-Institute*
949 *for Meteorology*, **349**.
950 Rossow, W. B., and R. A. Schiffer, 1991: Isccp Cloud Data Products. *Bulletin of the*
951 *American Meteorological Society*, **72,** 2-20.
952 Rossow, W. B., and Y. C. Zhang, 1995: Calculation of Surface and Top of
953 Atmosphere Radiative Fluxes from Physical Quantities Based on Isccp
954 Data Sets .2. Validation and First Results. *Journal of Geophysical Research-*
955 *Atmospheres*, **100,** 1167-1197.
956 Taylor, K. E., R. J. Stouffer, and G. A. Meehl, 2012: An Overview of Cmip5 and the
957 Experiment Design. *Bulletin of the American Meteorological Society*, **93,**
958 485-498.
959 van Vuuren, D. P., and Coauthors, 2011: The representative concentration
960 pathways: an overview. *Climatic Change*, **109,** 5-31.
961 Weaver, A. J., M. Eby, F. F. Augustus, and E. C. Wiebe, 1998: Simulated influence of
962 carbon dioxide, orbital forcing and ice sheets on the climate of the Last
963 Glacial Maximum. *Nature*, **394,** 847-853.
964 Weaver, A. J., and Coauthors, 2001: The UVic Earth System Climate Model: Model
965 description, climatology, and applications to past, present and future
966 climates. *Atmosphere-Ocean*, **39,** 361-428.
967 Willson, R. C., and H. S. Hudson, 1991: The Suns Luminosity over a Complete
968 Solar-Cycle. *Nature*, **351,** 42-44.
969 Yang, H., Q. Li, K. Wang, Y. Sun, and D. Sun, 2015: Decomposing the meridional
970 heat transport in the climate system. *Clim. Dyn.*, **44**, 2751–2768,
971 doi:10.1007/s00382-014-2380-5.

972

973

Appendix A1: GREB model equations

The GREB model has four primary prognostic equations given below and all variable names are listed and explained in Table A1. The surface temperature, T_{surf}, tendencies:

$$\gamma_{surf}\frac{dT_{surf}}{dt} = F_{solar} + F_{thermal} + F_{latent} + F_{sense} + F_{ocean} + F_{correct} \quad [A1]$$

The atmospheric layer temperature, T_{atmos}, tendencies:

$$\gamma_{atmos}\frac{dT_{atmos}}{dt} = -F_{sense} + Fa_{thermal} + Q_{latent} + \gamma_{atmos}(\kappa \cdot \nabla^2 T_{atmos} - \vec{u} \cdot \nabla T_{atmos}) \quad [A2]$$

The subsurface ocean temperature, T_{ocean}, tendencies:

$$\frac{dT_{ocean}}{dt} = \frac{1}{\Delta t}\Delta To_{entrain} - \frac{1}{\gamma_{ocean}-\gamma_{surf}}Fo_{sense} + Fo_{correct} \quad [A3]$$

The atmospheric specific humidity, q_{air}, tendencies:

$$\frac{dq_{air}}{dt} = \Delta q_{eva} + \Delta q_{precip} + \kappa \cdot \nabla^2 q_{air} - \vec{u} \cdot \nabla q_{air} + q_{correct} \quad [A4]$$

It should be noted here that heat transport is only within the atmospheric layer (eq. [A2]). Together with the moisture transport in eq. [A4] these transports are the only way in which grid points of the GREB model interact with each other in the horizontal directions.

The surface layer heat capacity, γ_{surf}, is constant over land points. For ocean points it follows the ocean mixed layer depth, h_{mld}, if T_{surf} is above a temperature range near freezing. Within a range below freezing it is a linear increasing function of T_{surf} and for T_{surf} below this range γ_{surf} the same as over land points. (see DF11).

The absorbed solar radiation, F_{solar}, is a function of the cloud cover, CLD, boundary condition and the surface albedo, α_{surf}:

$$F_{solar} = (1 - \alpha_{clouds}) \cdot \left(1 - \alpha_{surf}\right) \cdot S_0 \cdot r \quad [A5]$$

with the atmospheric albedo, $\alpha_{clouds} = 0.35 \cdot CLD$. α_{surf} is a global constant if T_{surf} is below or above a temperature range near freezing. Within this range it is a linear decreasing function of T_{surf}, (see DF11). The thermal radiation at the surface is

$$F_{thermal} = -\sigma T_{surf}^4 + \varepsilon_{atmos}\sigma T_{atmos-rad}^4 \quad [A6]$$

and the thermal radiation from the atmosphere is

$$Fa_{thermal} = \sigma T_{surf}^4 - 2\varepsilon_{atmos}\sigma T_{atmos-rad}^4 \quad [A7]$$

The emissivity of the atmosphere, ε_{atmos}, is a function of the cloud cover, CLD, the atmospheric water vapour, $viwv_{atmos}$, and the CO_2, CO_2^{topo}, concentration

$$\varepsilon_{atmos} = \frac{pe_8 - CLD}{pe_9} \cdot (\varepsilon_0 - pe_{10}) + pe_{10} \quad [A8]$$

with

$$\varepsilon_0 = pe_4 \cdot \left[pe_1 \cdot CO_2^{topo} + pe_2 \cdot viwv_{atmos} + pe_3\right] + pe_5 \cdot \left[pe_1 \cdot CO_2^{topo} + pe_3\right] + pe_6 \cdot \left[pe_2 \cdot viwv_{atmos} + pe_3\right] + pe_7 \quad [A9]$$

The first three terms in the eq. [A9] represent different spectral bands in which the thermal radiation of water vapour and the CO_2 are active. In the first term both are active, in the second only CO_2 and in the third only water vapour. The combined effect of eqs. [A8] and [A9] is that the sensitivity of the emissivity to CO_2 is depending on the presents of cloud cover and water vapour.

It is important to note that this log-function parametrization of the emissivity is an approximation developed in DF11 for 2xCO_2-concentration experiments. While the parametrization may be a good approximation for a wide range of the greenhouse gasses, it is likely to have limited skill in extreme variation of the greenhouse gasses. For instance, if all greenhouse gasses (CO_2 and water vapour) concentrations and cloud cover are zero then the emissivity of the atmospheric layer in eq. [A9] becomes -0.26. This is not a physically meaningful value and experiments in which all greenhouse gasses (CO_2 and water vapour) and cloud cover are zero need to be analysed with caution. The analysis section will discuss these limitations in these experiments.

Tables

Table 1: Processes (switches) controlled in the sensitivity experiment for the mean climate deconstruction. Indentation in the left column indicates processes switches are dependent on the switches above being ON.

Mean Climate Deconstruction	
Name	Description
Ice-albedo	controls surface albedo (α_{surf}) and heat capacity (γ_{surf}) at sea ice points as function of T_{surf}
Clouds	controls cloud cover climatology. OFF equals no clouds.
Oceans	controls F_{ocean} term in eq. [A1] and the heat capacity (γ_{surf}) off all ocean points. OFF equals no F_{ocean} and as γ_{surf} over land.
Atmosphere	controls sensible heat flux (F_{sense}) and the downward atmospheric thermal radiation term in eq. [A6].
Diffusion of Heat	controls diffusion of heat
Advection of Heat	controls advection of heat
CO_2	controls CO_2 concentration
Hydrological cycle	controls atmospheric humidity. OFF equals zero humidity
Diffusion of water vapour	controls diffusion of water vapour
Advection of water vapour	controls advection of water vapour
Model Corrections	controls model flux correction terms

Table 2: Processes (switches) controlled in the sensitivity experiment for the $2xCO_2$ response deconstruction. Indentation in the left column indicates processes switches are dependent on the switches above being ON.

$2xCO_2$ Response Deconstruction	
Boundary Conditions	
Name	Description
Topography (Observed)	controls topography effect on thermal radiation. OFF equals all land point on sea level.
Clouds (climatology)	controls cloud cover climatology. OFF equals 0.7 cloud cover everywhere.
Humidity (climatology)	controls the humidity constraint. OFF equals a control humidity 0.0052 [kg/kg] everywhere. Humidity can still respond to forcings.
Feedbacks/Processes	
Diffusion of Heat	controls diffusion of heat
Advection of Heat	controls advection of heat
Ice-albedo	controls surface albedo (α_{surf}) and heat capacity (γ_{surf}) at sea ice points as function of T_{surf}
Ocean heat uptake	controls F_{ocean} term in eq. [A1] and the heat capacity (γ_{surf}) off all ocean points. OFF equals no F_{ocean} and γ_{surf} of a 50m water column.
Hydrological cycle	controls atmospheric humidity. OFF equals zero humidity
Diffusion of water vapour	controls diffusion of water vapour
Advection of water vapour	controls advection of water vapour

Table 3: List of scenario experiments.

RCP CO_2-scenarios		
Name	length	Description
Historical	1850-2000	CO_2-concentration following the historical scenario
RCP8.5	2001-2100	CO_2-concentration following the RCP8.5 scenario
RCP6	2001-2100	CO_2-concentration following the RCP6 scenario
RCP4	2001-2100	CO_2-concentration following the RCP4 scenario
RCP3PD	2001-2100	CO_2-concentration following the RCP3PD scenario
A1B	2001-2100	CO_2-concentration following the A1B scenario
Idealized CO_2 concentrations		
Zero-CO_2	100yrs	zero CO_2 concentrations
0.5xCO_2	50yrs	140ppm CO_2 concentrations
2xCO_2	50yrs	560ppm CO_2 concentrations
4xCO_2	100yrs	1120ppm CO_2 concentrations
10xCO_2	100yrs	2800ppm CO_2 concentrations
2xCO_2 abrupt reverse	100yrs	as 2xCO_2 with an abrupt reverse to control after 30yrs
2xCO_2 wave	100yrs	CO_2 concentration oscillating with 30yrs period
Partial CO_2 concentrations		
CO_2-N-hemis	50yrs	2xCO_2 only in the northern hemisphere
CO_2-S-hemis	50yrs	2xCO_2 only in the southern hemisphere
CO_2-tropics	50yrs	2xCO_2 only between 30^{o}S and 30^{o}N
CO_2-extra-tropics	50yrs	2xCO_2 only poleward of 30^o
CO_2-oceans	50yrs	2xCO_2 only over ice-free ocean points
CO_2-land	50yrs	2xCO_2 only over land and sea ice points
CO_2-winter	50yrs	2xCO_2 only in the month Oct. to Mar.
CO_2-summer	50yrs	2xCO_2 only in the month Apr. to Sep.
Solar radiation		
solar+27W/m^2	50yrs	solar constant increased by +27W/m^2
11yrs-solar	50yrs	solar idealized solar constant 11yrs cycle
Orbital parameter		
Solar-231Kyr	100yrs	incoming solar radiation according to orbital parameters 231Kyrs ago.
Solar-231Kyr-200ppm	100yrs	as Solar-231Kyr, but with CO_2 concentrations decreased from 280ppm to 200ppm.
Orbit-radius	40steps	equilibrium response to different Earth orbit radius from 0.8AU to 1.2AU.
Obliquity	45steps	equilibrium response to different Earth axis tilt from -25 ^{o} to 90^o
Eccentricity	60steps	equilibrium response to different Earth orbit eccentricity from 0.3 to 0.3

Table A1: Variables of the GREB model equations.

Variable	Dimensions	Description
T_{surf}	x, y, t	surface temperature
T_{atmos}	x, y, t	atmospheric temperature
T_{ocean}	x, y, t	subsurface ocean temperature
q_{air}	x, y, t	atmospheric humidity
γ_{surf}	x, y, t	heat capacity of the surface layer
γ_{atmos}	x, y, t	heat capacity of the atmosphere
γ_{ocean}	x, y, t	heat capacity of the subsurface ocean
F_{solar}	x, y, t	solar radiation absorbed at the surface
$F_{thermal}$	x, y, t	thermal radiation into the surface
$Fa_{thermal}$	x, y, t	thermal radiation into the atmospheric
F_{latent}	x, y, t	latent heat flux into the surface
Q_{latent}	x, y, t	latent heat flux into the atmospheric
F_{sense}	x, y, t	sensible heat flux from the atmosphere into the surface
Fo_{sense}	x, y, t	sensible heat flux from the subsurface ocean into the surface layer
F_{ocean}	x, y, t	sensible heat flux from the subsurface ocean
$F_{correct}$	x, y, t	heat flux corrections for the surface
$Fo_{correct}$	x, y, t	heat flux corrections for the subsurface ocean
$q_{correct}$	x, y, t	mass flux corrections for the atmospheric humidity
$\Delta To_{entrain}$	x, y, t	subsurface ocean temperature tendencies by entrainment
Δq_{eva}	x, y, t	mass flux for the atmospheric humidity by evaporation
Δq_{precip}	x, y, t	mass flux for the atmospheric humidity by precipitation
α_{surf}	x, y, t	albedo of the surface layer
ε_{atmos}	x, y, t	emissivity of the atmosphere
$T_{atmos-rad}$	x, y, t	atmospheric radiation temperature
$viwv_{atmos}$	x, y, t	atmospheric column water vapour mass
κ	constant	isotropic diffusion coefficient
pe_i	constant	empirical emissivity function parameters
$\vec{u}$	x, y, t_j	horizontal wind field
α_{clouds}	x, y, t_j	albedo of the atmosphere
h_{mld}	x, y, t_j	Ocean mixed layer depth
r	y, t_j	fraction of incoming sunlight (24hrs average)
CO_2^{topo}	x, y	CO_2 concentration scaled by topographic elevation
S_0	constant	solar constant
σ	constant	Stefan-Bolzman constant
t_j	-	day within the annual calendar
Δt	constant	model integration time step
σ	constant	Stefan-Boltzmann constant

Figures

Figure 1. MSCM interface running the deconstruction of the mean climate experiments. The experiment A, on the left, has all processes turned ON and experiment B, on right, has all turned OFF. The T_{surf} of Experiment A is shown in the upper left map, Exp. B in the upper right and the difference between both in the lower map. The example shows the values for the October mean.

Figure 2. MSCM interface running the deconstruction of the response to a doubling of the CO_2 concentration experiments. The experiment A, on the left, has all processes turned ON and experiment B, on right, has all turned OFF. The T_{surf} response of Experiment A is shown in the upper left map, Exp. B in the upper right and the difference between both in the lower map. The example shows the annual mean values after 28yrs.

Figure 3. Examples of the MSCM scenario interface. (a) presenting a single scenario (here RCP 8.5 CO_2 forcing) and (b) the comparison of two different scenarios (here a CO_2 forcing is compared against a change in the solar constant by +27W/m^2).

Figure 4. T_{surf} annual mean (upper row) and seasonal cycle (half the difference between mean of July to September minus January to March; middle row) for the GREB experiment with all processes turned OFF (Bare Earth), only the correction term OFF (GREB) and observed (identical to GREB with all processes on) are shown. The zonal mean of the annual mean (g) and seasonal cycle (h) of the experiments and observations in comparison with the zonal mean RMSE of the GREB model without correction terms relative to observed are shown.

Figure 5. Changes in the annual mean T_{surf} in the GREB model simulations with different processes turned OFF as described in section 2a relative to the complete GREB model without model correction terms: (a) Ice/Snow, (b) clouds, (c) oceans, (d) heat advection, (e) heat diffusion, (f) CO_2 concentration, (g) hydrological cycle, (h) diffusion of water vapour and (i) advection of water vapour. Global mean differences are shown in the headings. Differences are for the control minus the sensitivity experiment (positive indicates the control experiment is warmer). All values are in ^oC. In some panels, the values are scaled for better comparison: (b), (c) and (f) by a factor of 2, (a), (d) and (e) by a factor of 3, and (h) and (i) by a factor of 6.

Figure 6. As in Fig. 5, but for the seasonal cycle. The mean seasonal cycle is defined by the difference between the month [JAS] - [JFM] divided by two. Positive values on the North hemisphere indicate stronger seasonal cycle in the sensitivity experiments than in the full GREB model. Vice versa for the Southern Hemisphere. Global root mean square differences are shown in the headings. All values are in ^oC. In some panels, the values are scaled for better comparison: (b), (d) and (e) by a factor of 2, and (h) and (i) by a

factor of 10. (g) is the mean for the hydrological cycle experiments with and without the ice-albedo process active.

Figure 7. Zonal mean values of the annual mean (a) and seasonal cycle differences (b) for the experiments as shown in Figs. 5 and 6. g) The mean for the hydrological cycle is for the experiments with and without the ice-albedo process active.

Figure 8. Conceptual build-up of the annual mean climate: staring with all processes turned OFF (a) and then adding more processes in each row: (b) atmosphere, (d) CO_2, (f) oceans, (h) heat diffusion, (j) heat advection, (l) hydrological cycle, (n) ice-albedo, (p) clouds and (r) water vapour transport. The panels on the right column show the difference of the left panel to the previous row left panel. Global mean values are shown in the heading. All values are in ^oC. In some panels in the right column the values are scaled for better comparison: (e), (g) and (q) by a factor of 2, (i) by a factor of 3 and (k), (o) and (s) by a factor of 4. For details see on the experiments see section 2a.

Figure 9. As in Fig. 8, but conceptual build-up of the seasonal cycle. The seasonal cycle is defined by the difference between the month [JAS] - [JFM] divided by two. Global mean absolute values are shown in the heading. In some panels in the right column the values are scaled for better comparison: (c), (i), (m) and (o) by a factor of 2, (k), (q) and (s) by a factor of 5 and for (e) by a factor of 30.

Figure 10. Local T_{surf} response to doubling of the CO_2 concentration in experiments without atmospheric transport (each point on the maps is independent of the others). (a) GREB with topography, humidity and cloud processes and all other processes OFF. (b) Difference of (a) to GREB with topography and all other processes OFF scaled by a factor of 10. (c) GREB model as in (a), but with ice-albedo process ON. (d) Difference of (c)-(a) scaled by a factor of 2. (e) GREB model as in (a), but with hydrological cycle process ON. (f) Difference of (e)-(a) scaled by a factor of 2. For details see on the experiments see section 2b.

Figure 11. Global mean T_{surf} response to idealized forcing scenarios: (a) different RCP CO_2 forcing scenarios. (b) Scaled CO_2 concentrations. (c) idealized CO_2 concentration time evolutions (dotted lines) and the respective T_{surf} responses (solid lines of the same colour) for the $2xCO_2$ abrupt reverse (red) and the $2xCO_2$ wave (blue) simulations. (d) idealized 11yrs solar cycle. List of experiments is given in Table 3.

Figure 12. T_{surf} response to partial doubling of the CO_2 concentration in: Northern (a) and Southern (b) hemisphere, tropics (d) and extra-tropics (e), oceans (g) and land (h), and in boreal winter (j) and summer (k) . The right column panels show the difference between the two panels two the left in the same row.

Figure 13. T_{surf} response to changes in the solar constant by +27W/m^2 (middle column) versus a doubling of the CO_2 concentration (left column) for the annual mean (upper) and the seasonal cycle (lower). The seasonal cycle is defined by the difference between the month [JAS] - [JFM] divided by two. The right column panels show the difference between the two panels two the left in the same row scaled by 4 (c) and 3 (f).

Figure 14. Orbital parameter forcings and T_{surf} responses: (a) incoming solar radiation changes in the Solar-231Kyr experiment relative to the control GREB model. T_{surf} response in Solar-231Kyr (b) and Solar-231Kyr-200ppm (c) relative to the control GREB model. Annual mean T_{surf} in Orbit-radius (d), Obliquity (e) and Eccentricity (f). The solid vertical line in (d)-(f) marks the control (today) GREB model.

Supplementary Figures

SFigure 1. Changes in the annual mean T_{surf} in the GREB model simulations with different processes turn OFF as in Fig. 5 but relative to the complete GREB model without model correction terms and without Ice/Snow: (a) undefined, (b) clouds, (c) oceans, (d) heat advection, (e) heat diffusion, (f) CO_2 concentration, (g) hydrological cycle, (h) diffusion of water vapour and (i) advection of water vapour. Global mean differences are shown in the headings. All values are in ^oC. In some panels, the values are scaled for better comparison: (a), (d) and (e) by a factor of 2, and (h) and (i) by a factor of 5.

SFigure 2. Conceptual build-up of the annual mean climate as in Fig. 8. Panels (a) to (c) as in fig.8. (d) with the atmospheric emissivity set to zero, and (f) with the emissivity set 0.01. The panels on the right column show the difference of the left panel to (a). Global mean values are shown in the heading. All values are in ^oC. In the right column, the values are scaled by a factor of 2 for better comparison. For details see on the experiments see section 2a.

Figure 1

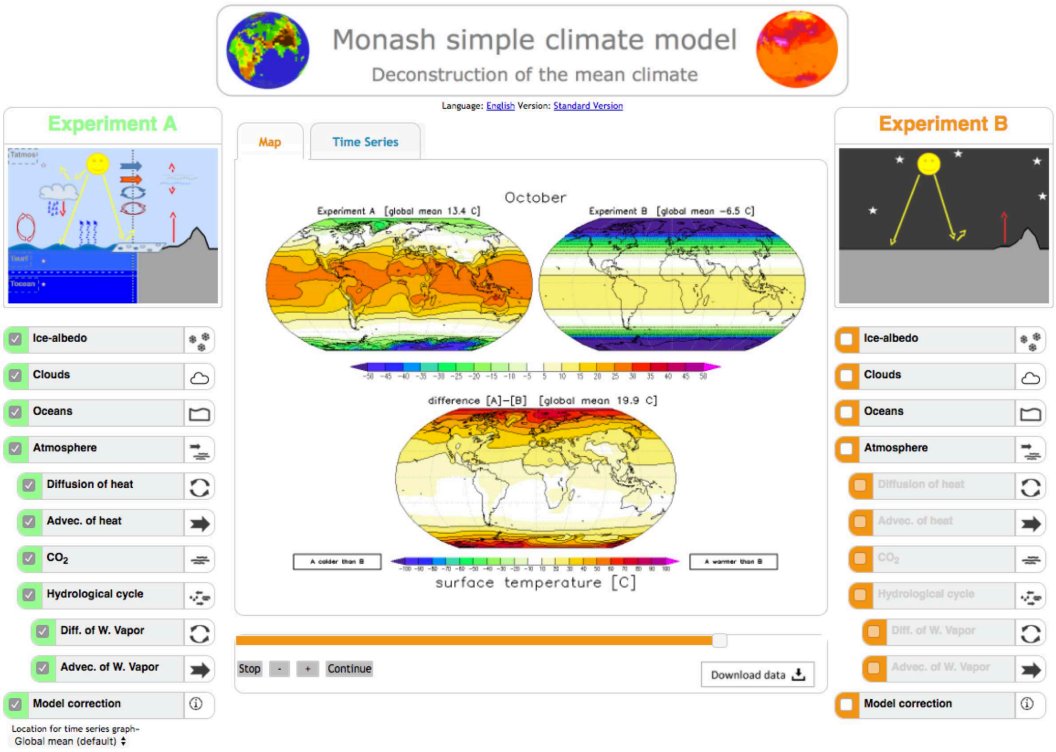

Figure 1: MSCM interface running the deconstruction of the mean climate experiments. The experiment A, on the left, has all processes turned ON and experiment B, on right, has all turned OFF. The T_{surf} of Experiment A is shown in the upper left map, Exp. B in the upper right and the difference between both in the lower map. The example shows the values for the October mean.

Figure 2

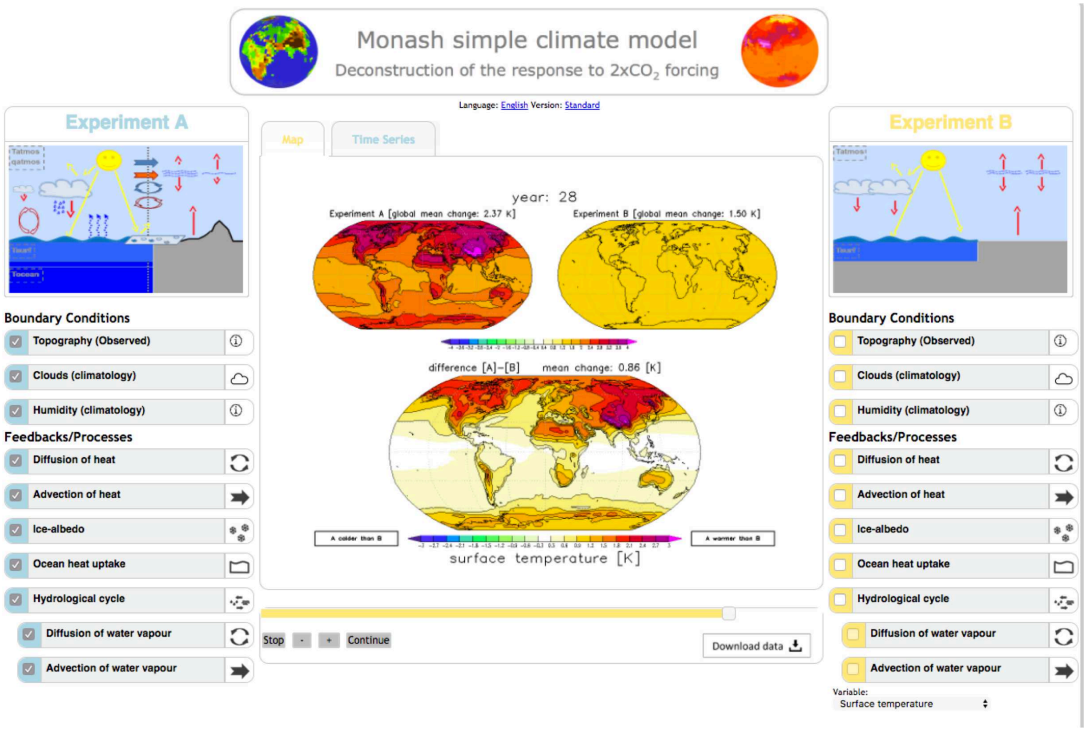

Figure 2: MSCM interface running the deconstruction of the response to a doubling of the CO_2 concentration experiments. The experiment A, on the left, has all processes turned ON and experiment B, on right, has all turned OFF. The T_{surf} response of Experiment A is shown in the upper left map, Exp. B in the upper right and the difference between both in the lower map. The example shows the annual mean values after 28yrs.

Figure 3

(a)

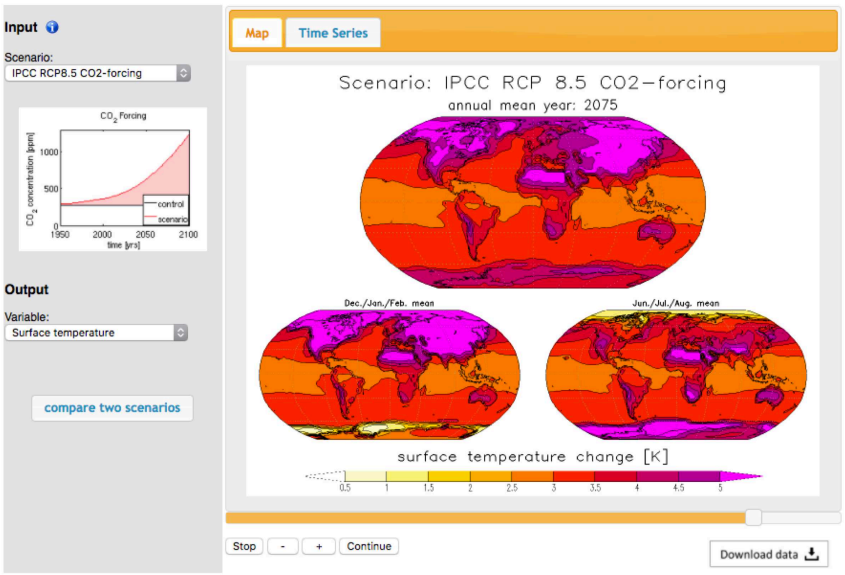

(b)

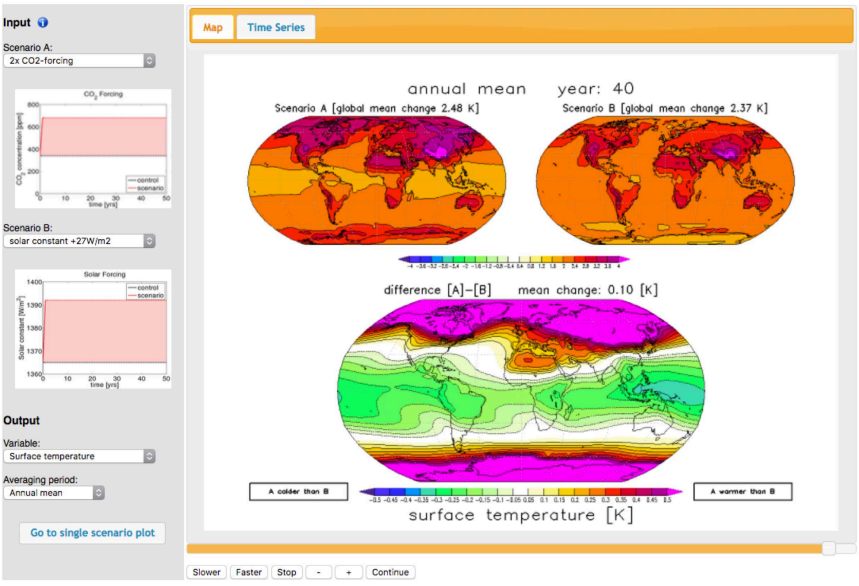

Figure 3: Examples of the MSCM scenario interface. (a) presenting a single scenario (here RCP 8.5 CO_2 forcing) and (b) the comparison of two different scenarios (here a CO_2 forcing is compared against a change in the solar constant by $+27W/m^2$).

Figure 4

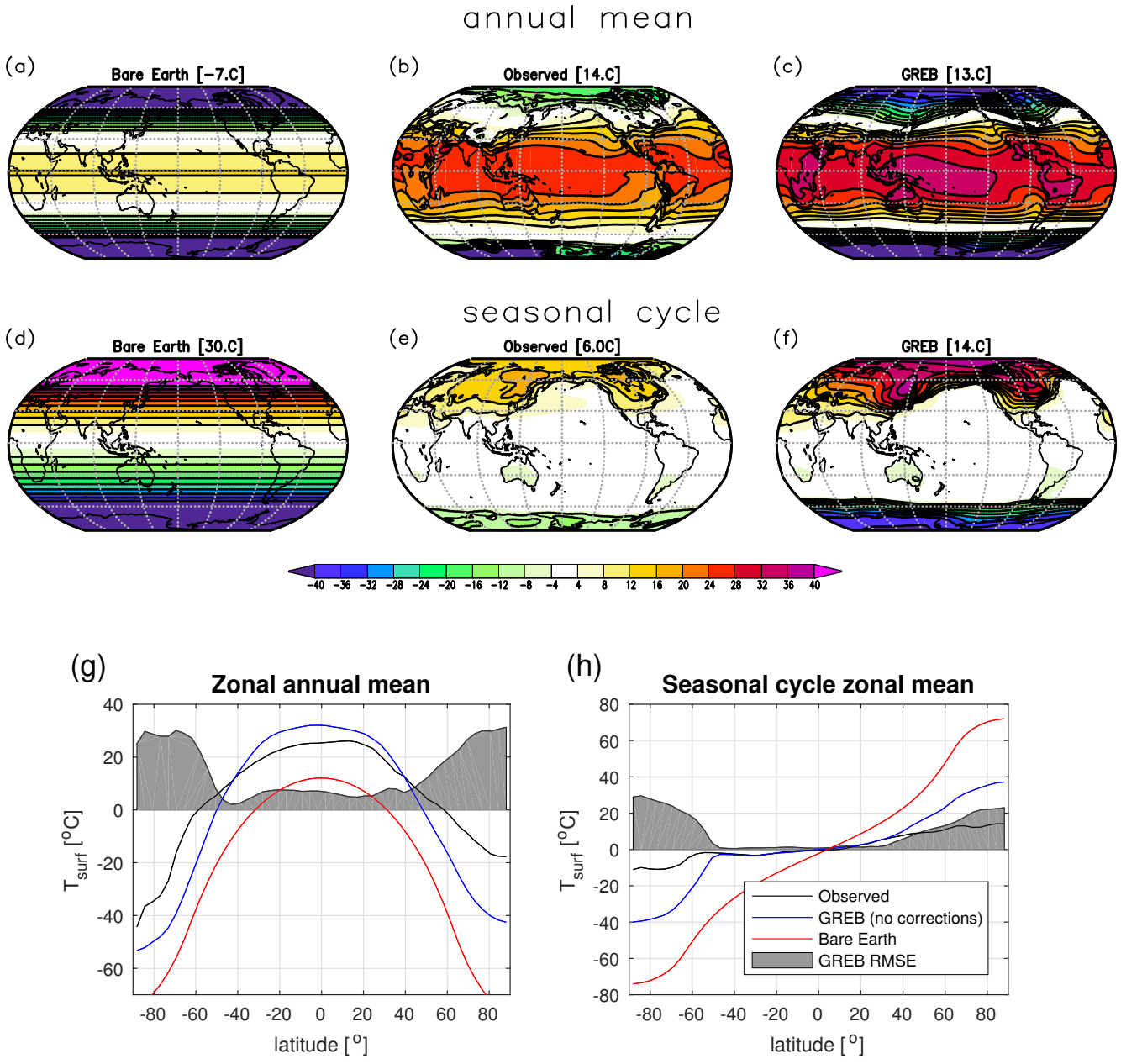

Figure 4: Tsurf annual mean (upper row) and seasonal cycle (half the difference between mean of July to September minus January to March; middle row) for the GREB experiment with all processes turned OFF (Bare Earth), only the correction term OFF (GREB) and observed (identical to GREB with all processes on) are shown. The zonal mean of the annual mean (g) and seasonal cycle (h) of the experiments and observations in comparison with the zonal mean RMSE of the GREB model without correction terms relative to observed are shown.

Figure 5

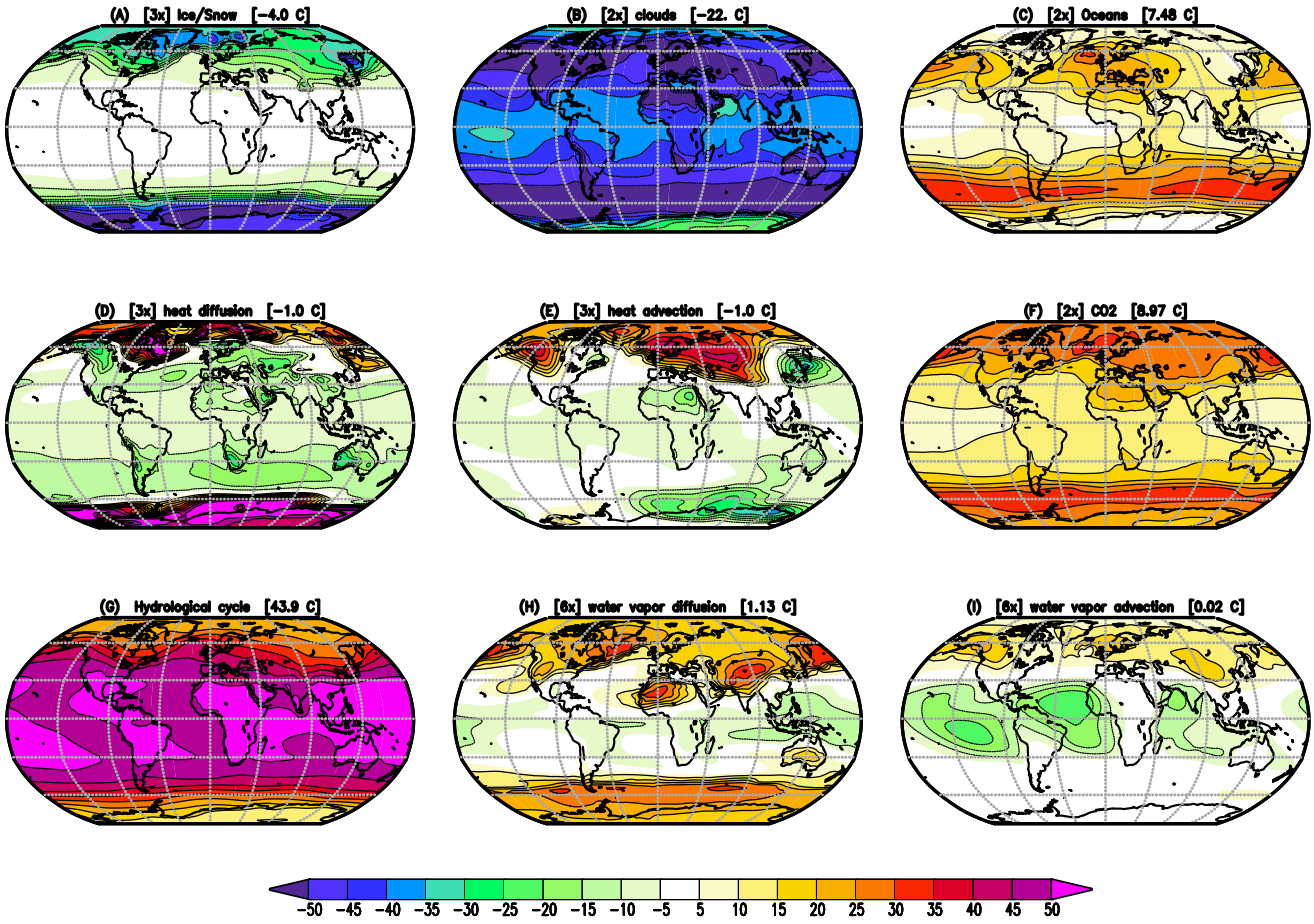

Figure 5: Changes in the annual mean T_{surf} in the GREB model simulations with different processes turned OFF as described in section 2a relative to the complete GREB model without model correction terms: (a) Ice/Snow, (b) clouds, (c) oceans, (d) heat advection, (e) heat diffusion, (f) CO_2 concentration, (g) hydrological cycle, (h) diffusion of water vapour and (i) advection of water vapour. Global mean differences are shown in the headings. Differences are for the control minus the sensitivity experiment (positive indicates the control experiment is warmer). All values are in ^oC. In some panels, the values are scaled for better comparison: (b), (c) and (f) by a factor of 2, (a), (d) and (e) by a factor of 3, and (h) and (i) by a factor of 6.

Figure 6

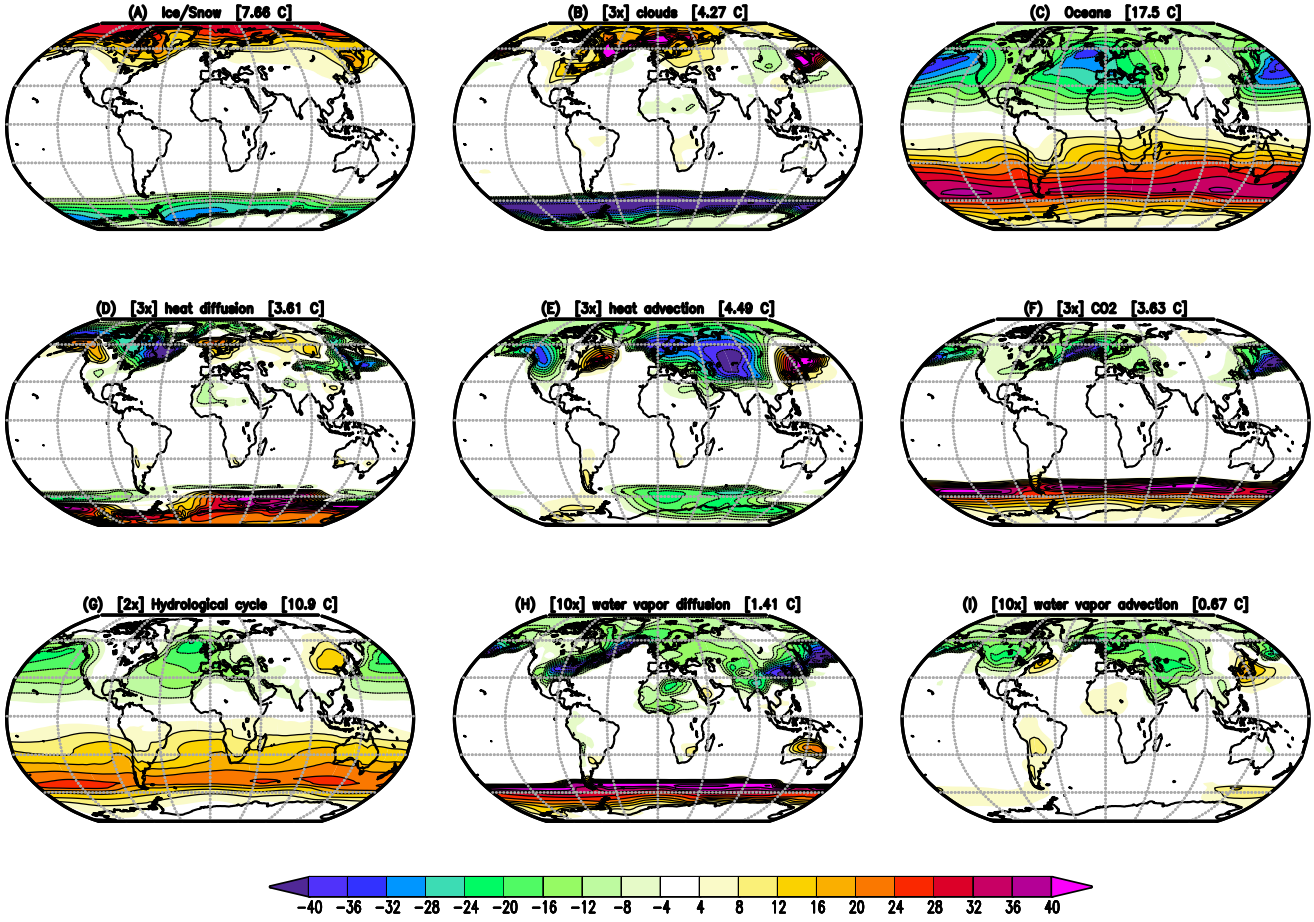

Figure 6: As in Fig. 5, but for the seasonal cycle. The mean seasonal cycle is defined by the difference between the month [JAS] - [JFM] divided by two. Positive values on the North hemisphere indicate stronger seasonal cycle in the sensitivity experiments than in the full GREB model. Vice versa for the Southern Hemisphere. Global root mean square differences are shown in the headings. All values are in ^oC. In some panels, the values are scaled for better comparison: (b), (d) and (e) by a factor of 2, and (h) and (i) by a factor of 10. (g) is the mean for the hydrological cycle experiments with and without the ice-albedo process active.

Figure 7

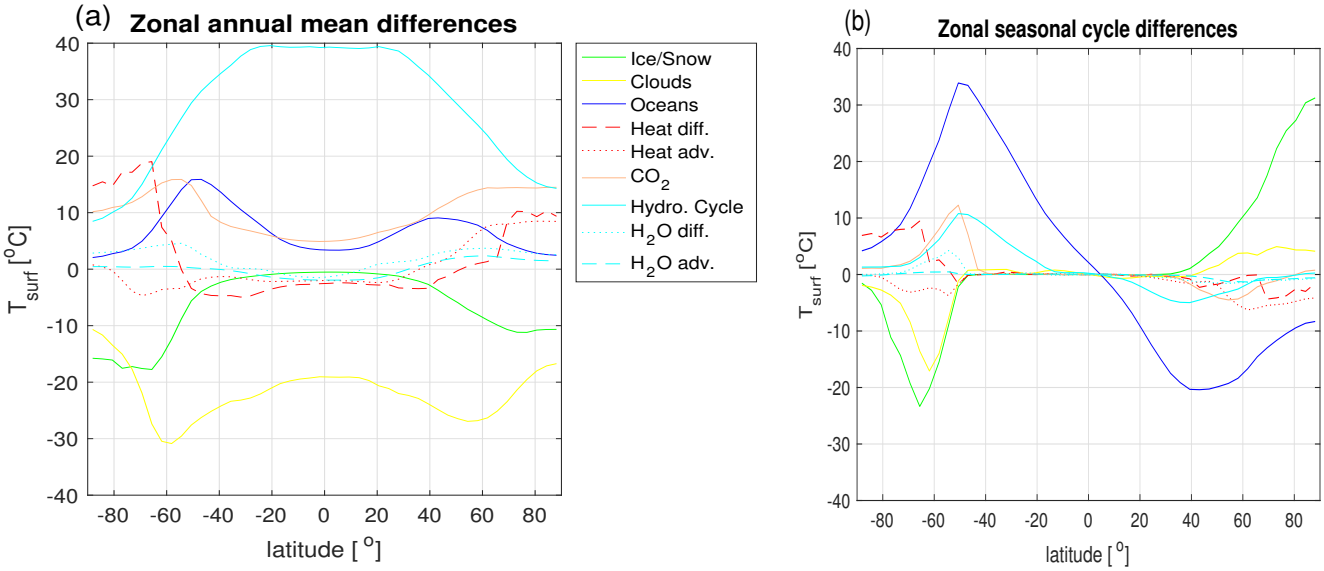

Figure 7: Zonal mean values of the annual mean (a) and seasonal cycle differences (b) for the experiments as shown in Figs. 5 and 6. g) The mean for the hydrological cycle is for the experiments with and without the ice-albedo process active.

Figure 8 part 1

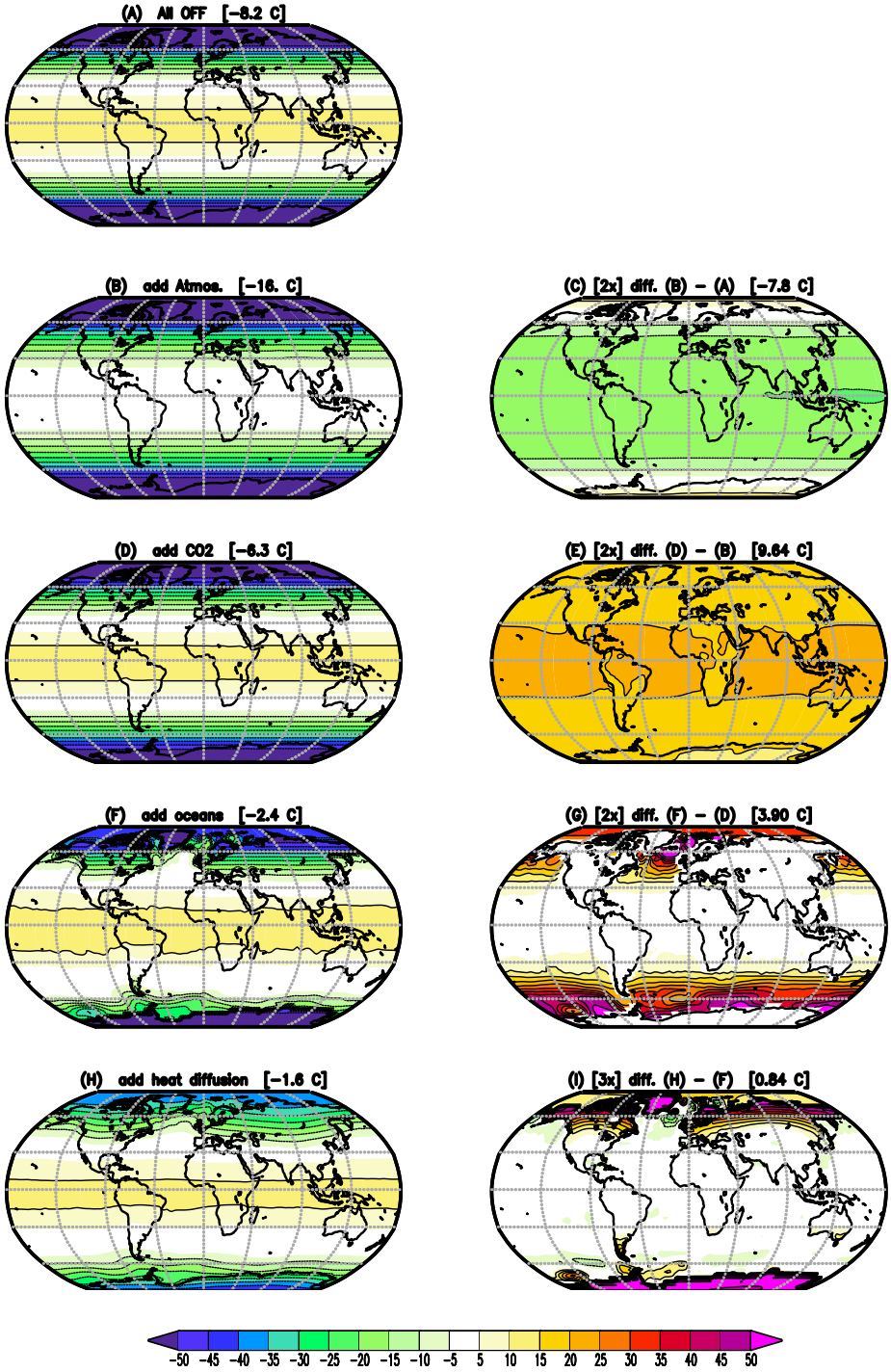

Figure 8: Conceptual build-up of the annual mean climate: staring with all processes turned OFF (a) and then adding more processes in each row: (b) atmosphere, (d) CO2, (f) oceans, (h) heat diffusion, (j) heat advection, (l) ice-albedo, (n) hydrological cycle, (p) clouds and (r) water vapour transport. The panels on the right column show the difference of the left panel to the previous row left panel. Global mean values are shown in the heading. All values are in oC. In some panels in the right column the values are scaled for better comparison: (e), (g) and (q) by a factor of 2, (i) and (m) by a factor of 3 and (c), (k) and (s) by a factor of 4. For details see on the experiments see section 2a.

Figure 8 part 2

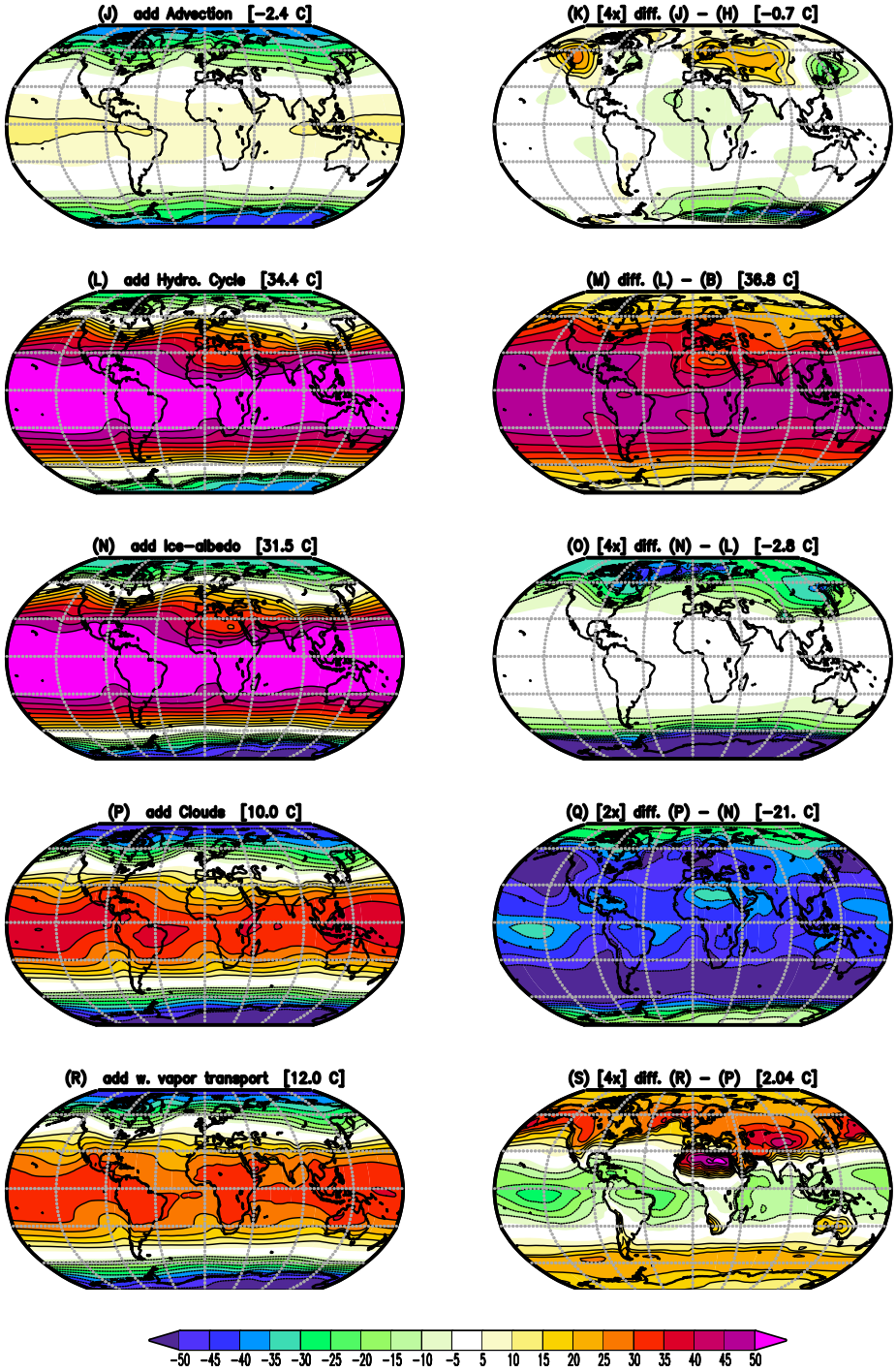

Figure 9 part 1

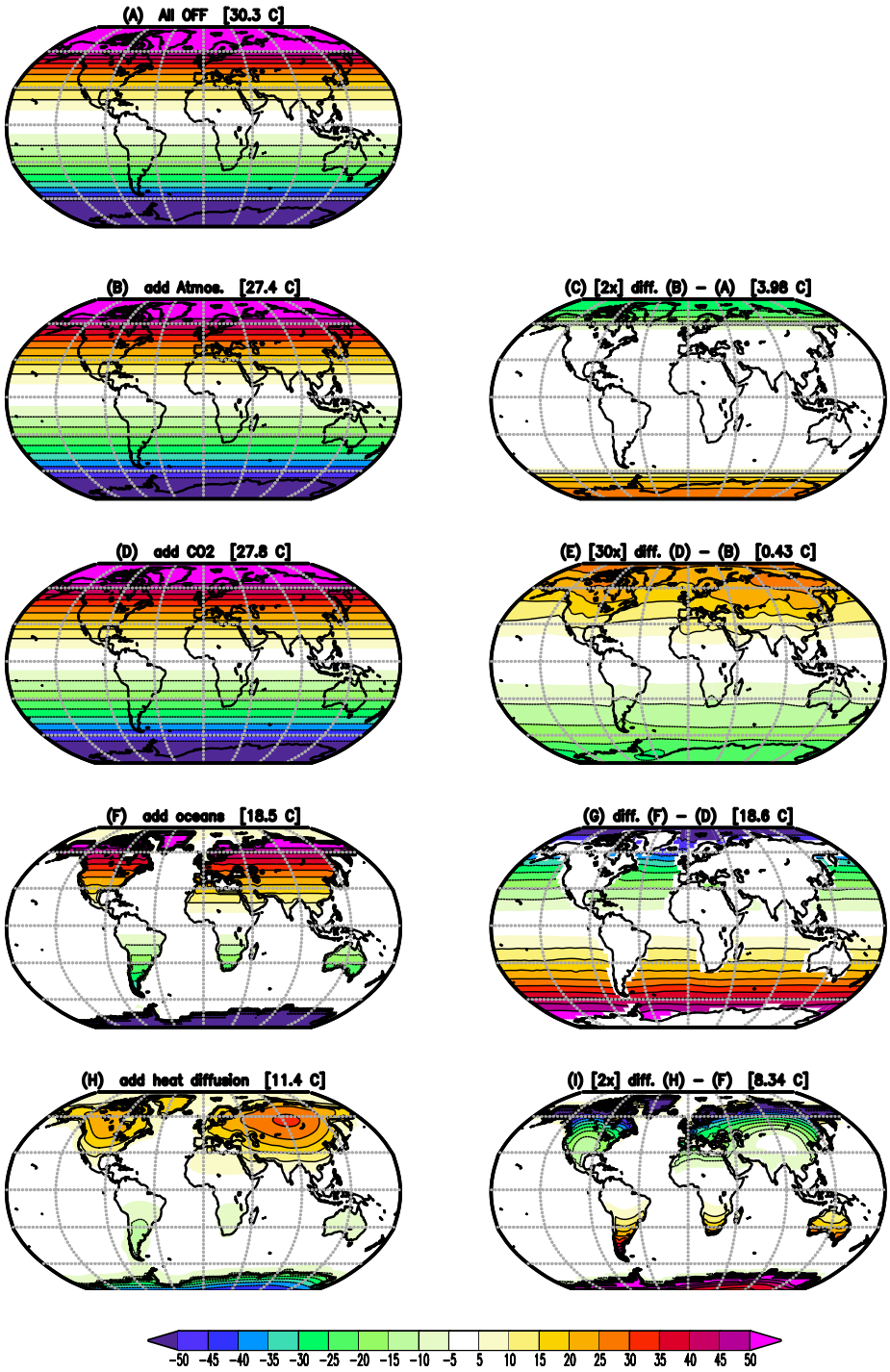

Figure 9: As in Fig. 8, but conceptual build-up of the seasonal cycle. The seasonal cycle is defined by the difference between the month [JAS] - [JFM] divided by two. Global mean absolute values are shown in the heading. In some panels in the right column the values are scaled for better comparison: (c) and (o) by a factor of 2, (i), (k), (q) and (s) by a factor of 5 and for (e) by a factor of 30.

Figure 9 part 2

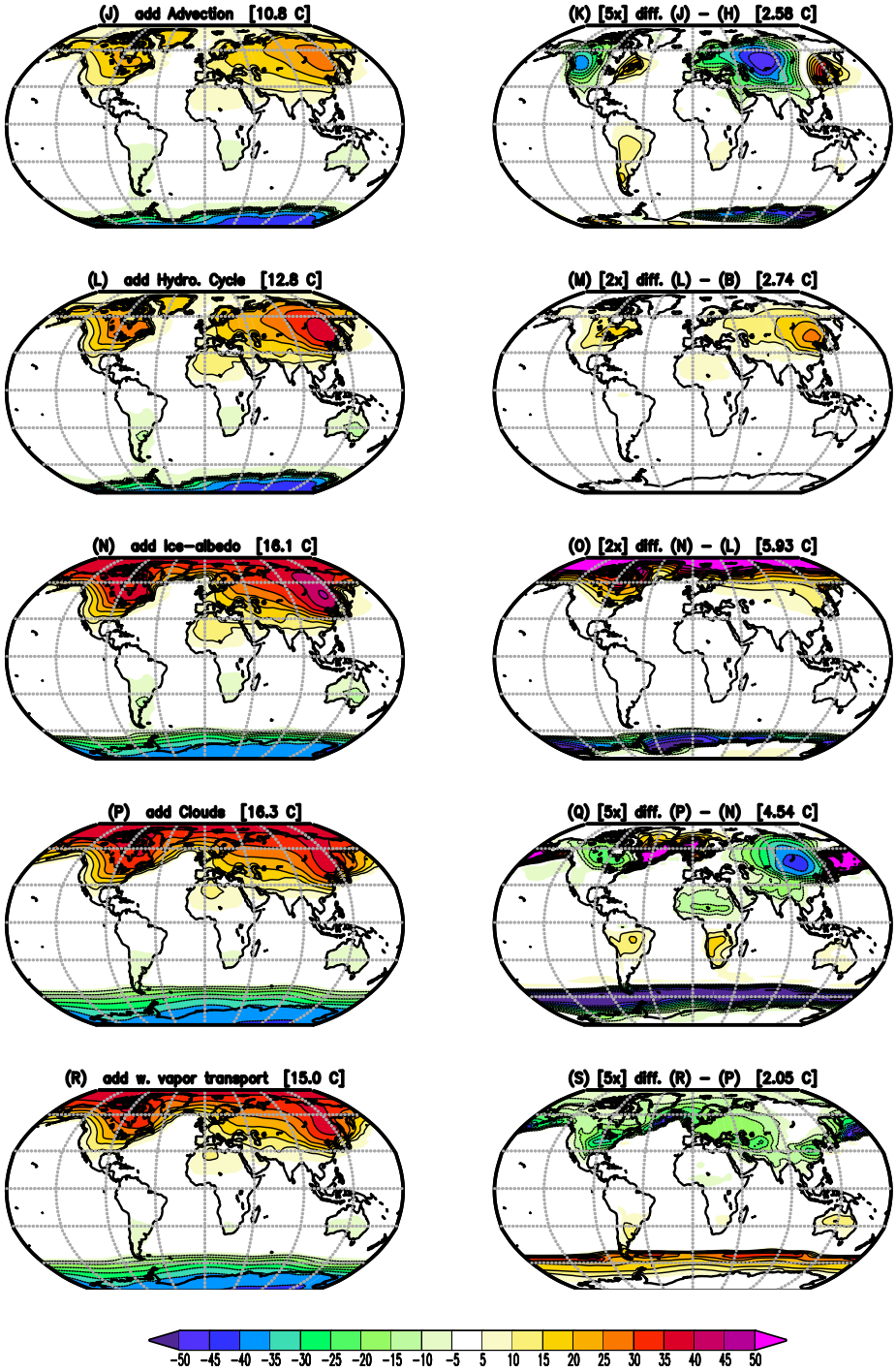

Figure10

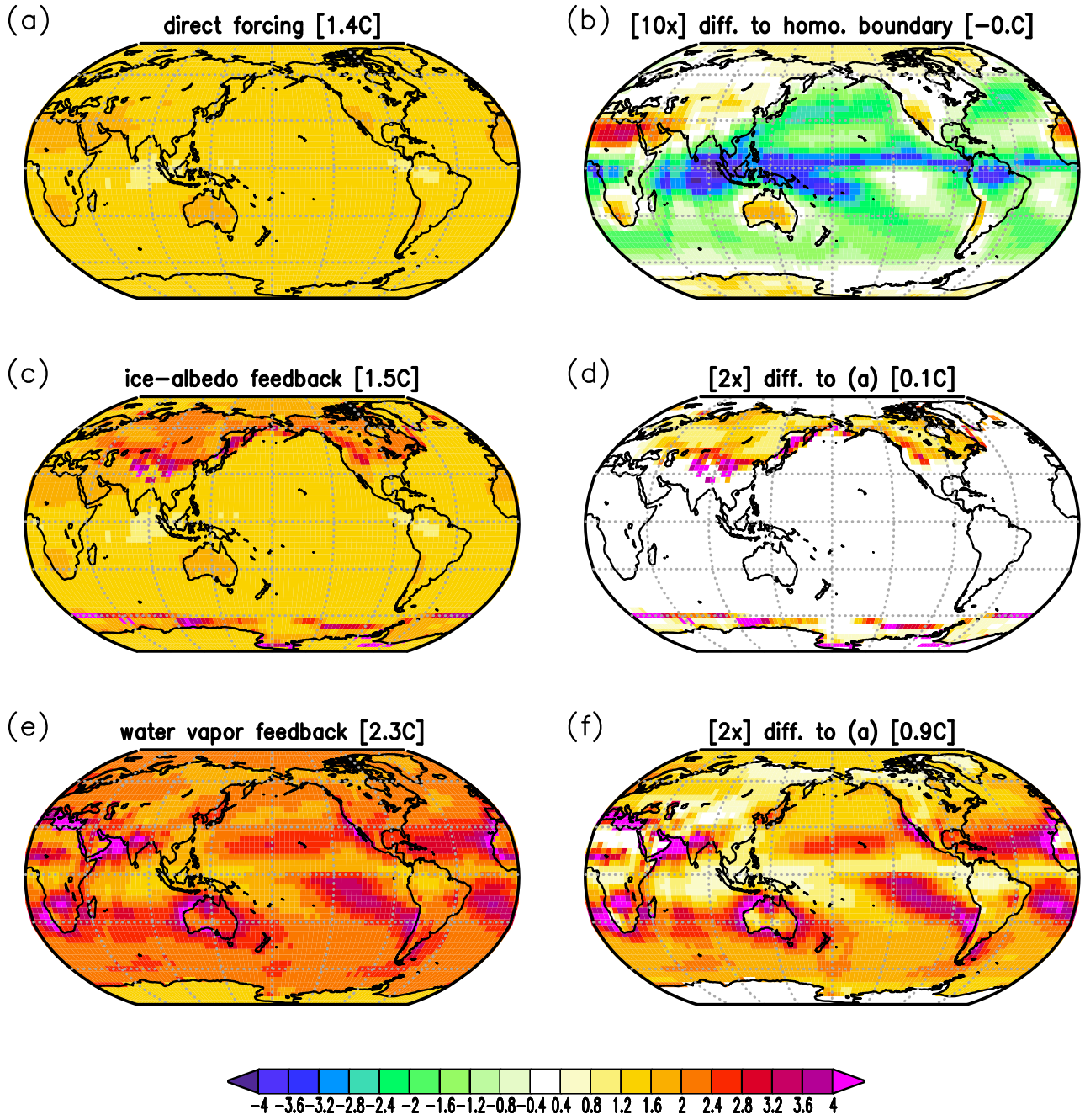

Figure 10: Local T_{surf} response to doubling of the CO_2 concentration in experiments without atmospheric transport (each point on the maps is independent of the others). (a) GREB with topography, humidity and cloud processes and all other processes OFF. (b) difference of (a) to GREB with topography and all other processes OFF scaled by a factor of 10. (c) GREB model as in (a), but with ice-albedo process ON. (d) difference of (c)-(a) scaled by a factor of 2. (e) GREB model as in (a), but with hydrological cycle process ON. (f) difference of (e)-(a) scaled by a factor of 2. For details see on the experiments see section 2b.

Figure 11

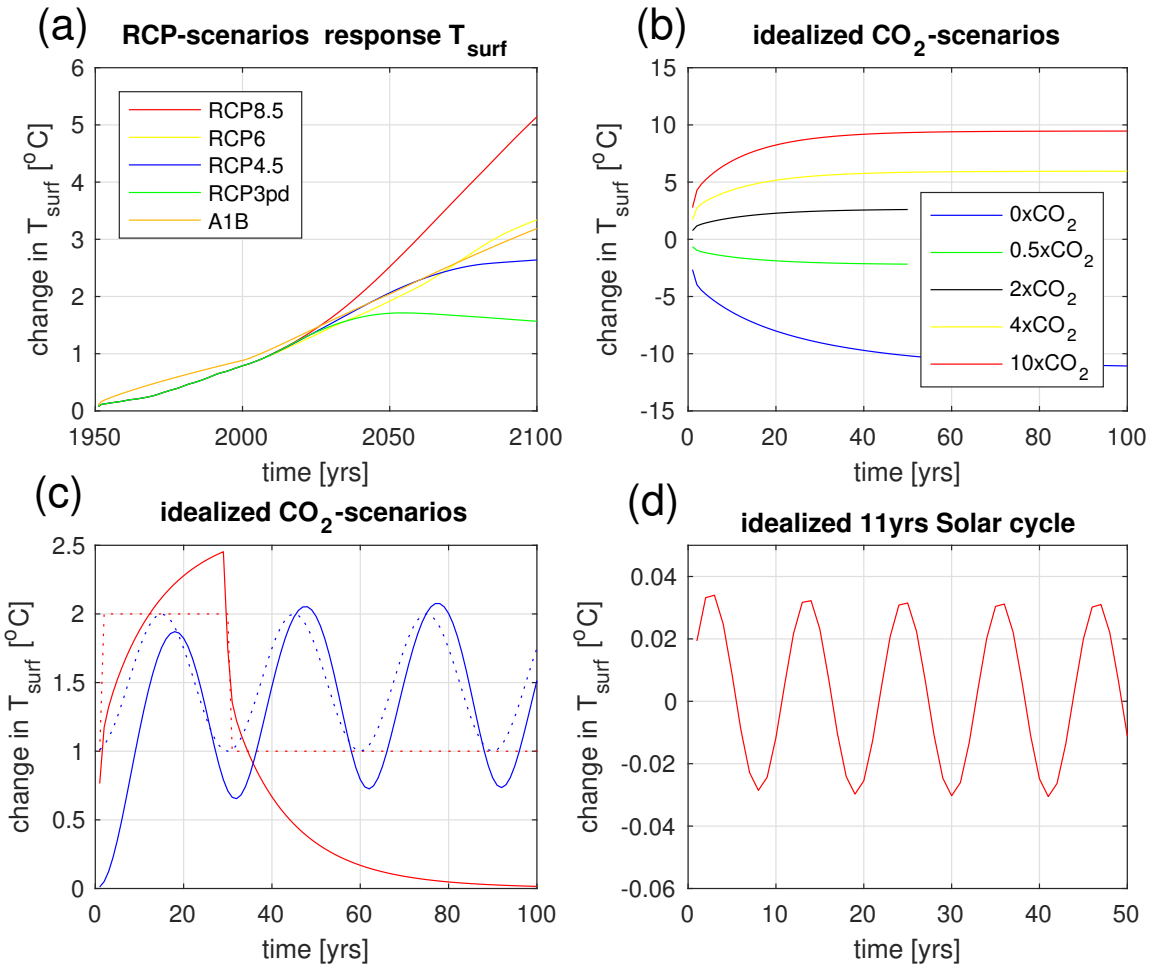

Figure 11: Global mean Tsurf response to idealized forcing scenarios: (a) different RCP CO2 forcing scenarios. (b) Scaled CO2 concentrations. (c) idealized CO2 concentration time evolutions (dotted lines) and the respective Tsurf responses (solid lines of the same colour) for the 2xCO2 abrupt reverse (red) and the 2xCO2 wave (blue) simulations. (d) idealized 11yrs solar cycle. List of experiments is given in Table 3.

Figure 12

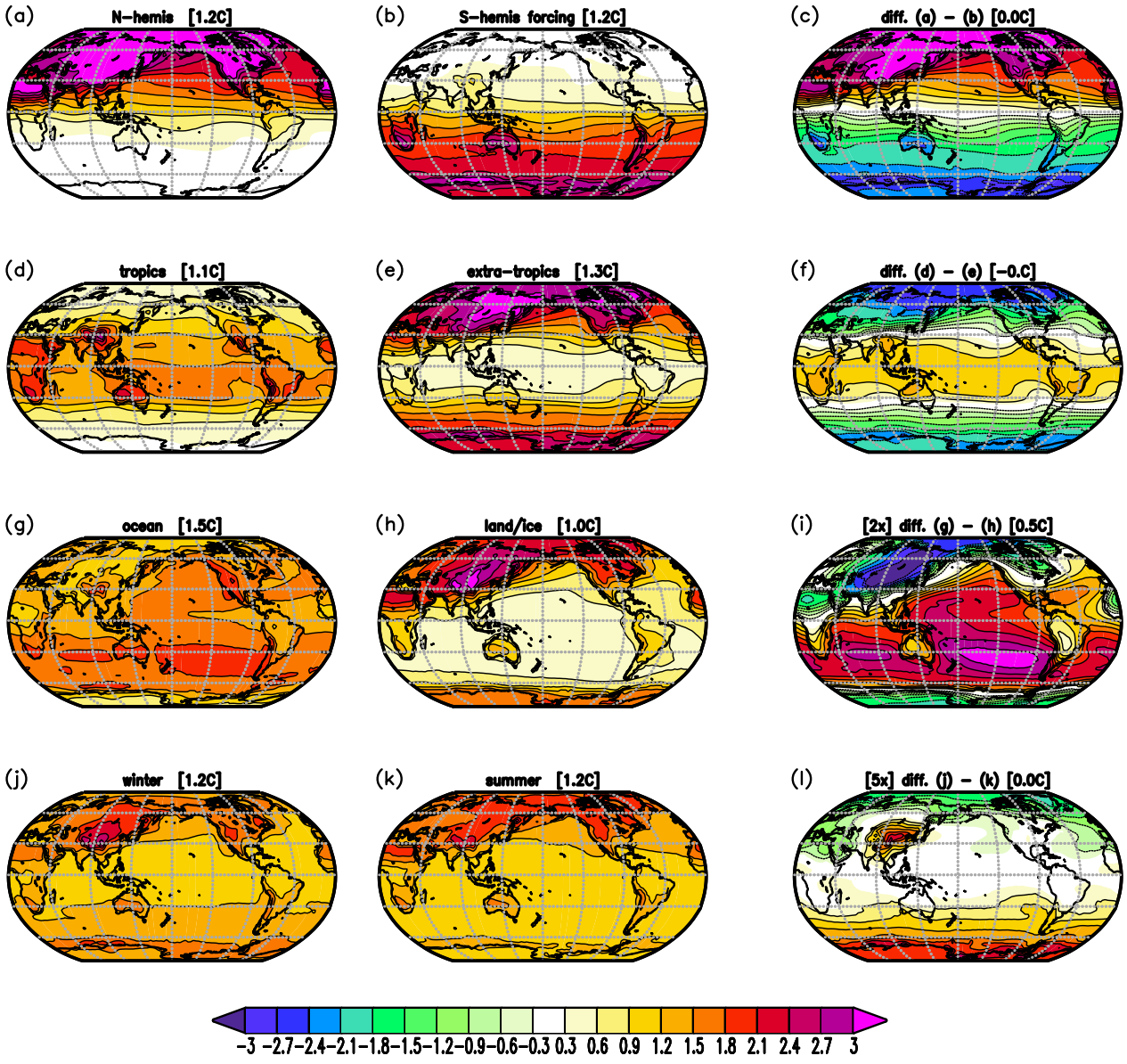

Figure 12: Tsurf response to partial doubling of the CO2 concentration in: Northern (a) and Southern (b) hemisphere, tropics (d) and extra-tropics (e), oceans (g) and land (h), and in boreal winter (j) and summer (k) . The right column panels show the difference between the two panels two the left in the same row.

Figure 13

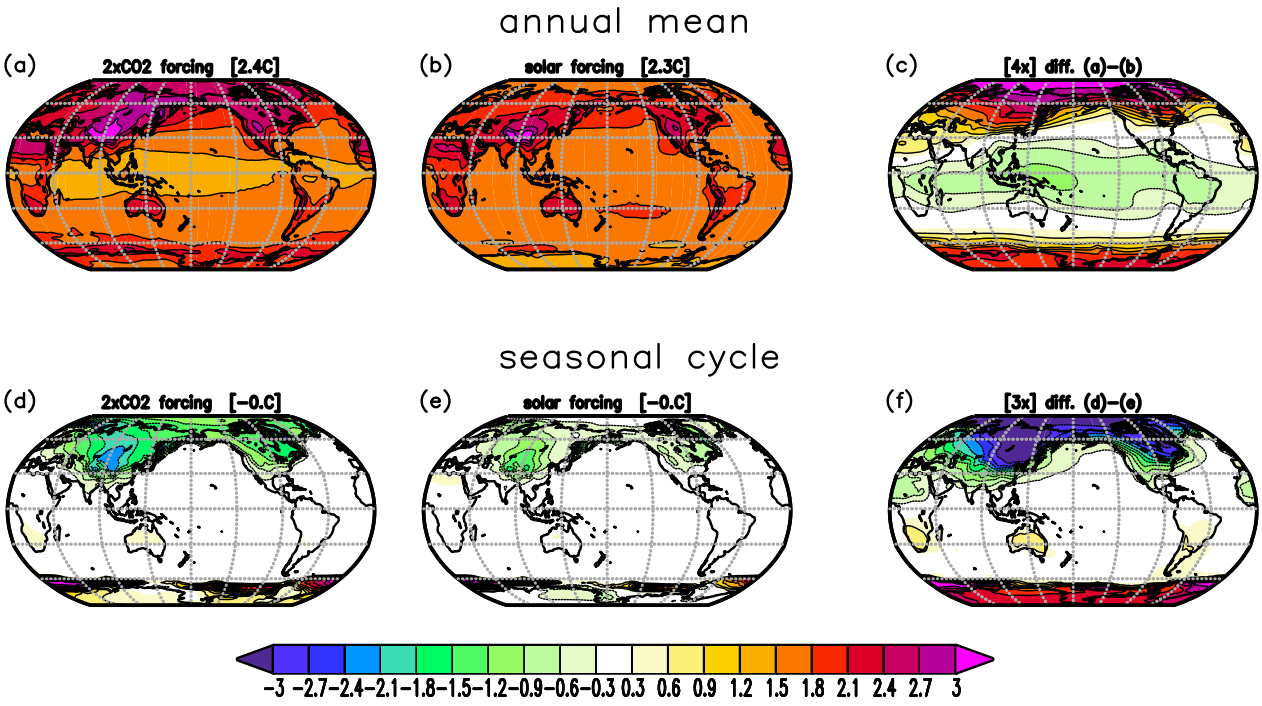

Figure 13: Tsurf response to changes in the solar constant by $+27 W/m^2$ (middle column) versus a doubling of the CO_2 concentration (left column) for the annual mean (upper) and the seasonal cycle (lower). The seasonal cycle is defined by the difference between the month [JAS] - [JFM] divided by two. The right column panels show the difference between the two panels two the left in the same row scaled by 4 (c) and 3 (f).

Figure 14

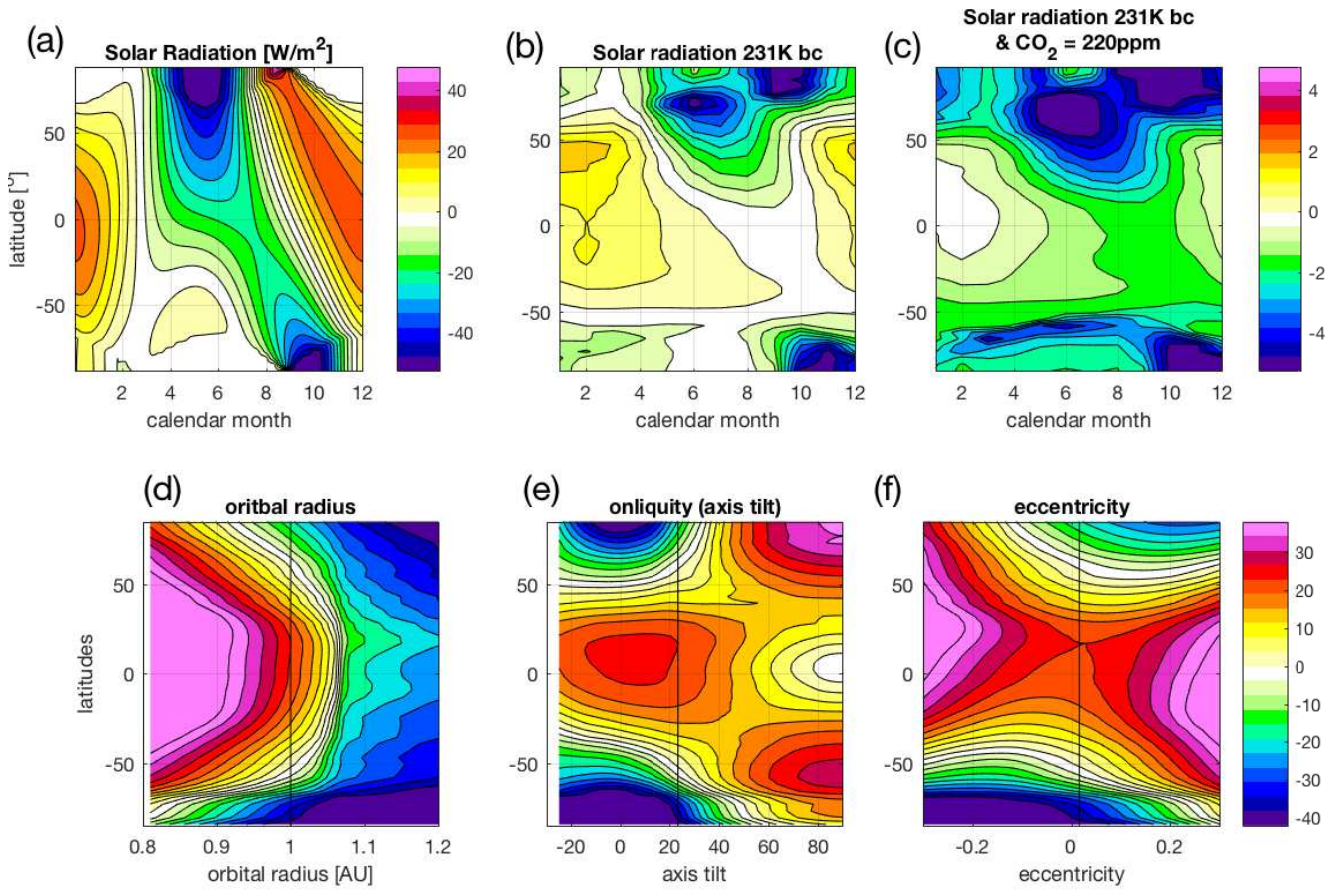

Figure 14: Orbital parameter forcings and Tsurf responses: (a) incoming solar radiation changes in the Solar-231Kyr experiment relative to the control GREB model. Tsurf response in Solar-231Kyr (b) and Solar-231Kyr-200ppm (c) relative to the control GREB model. Annual mean Tsurf in Orbit-radius (d), Obliquity (e) and Eccentricity (f). The solid vertical line in (d)-(f) marks the control (today) GREB model.

Supplementary Figure 1

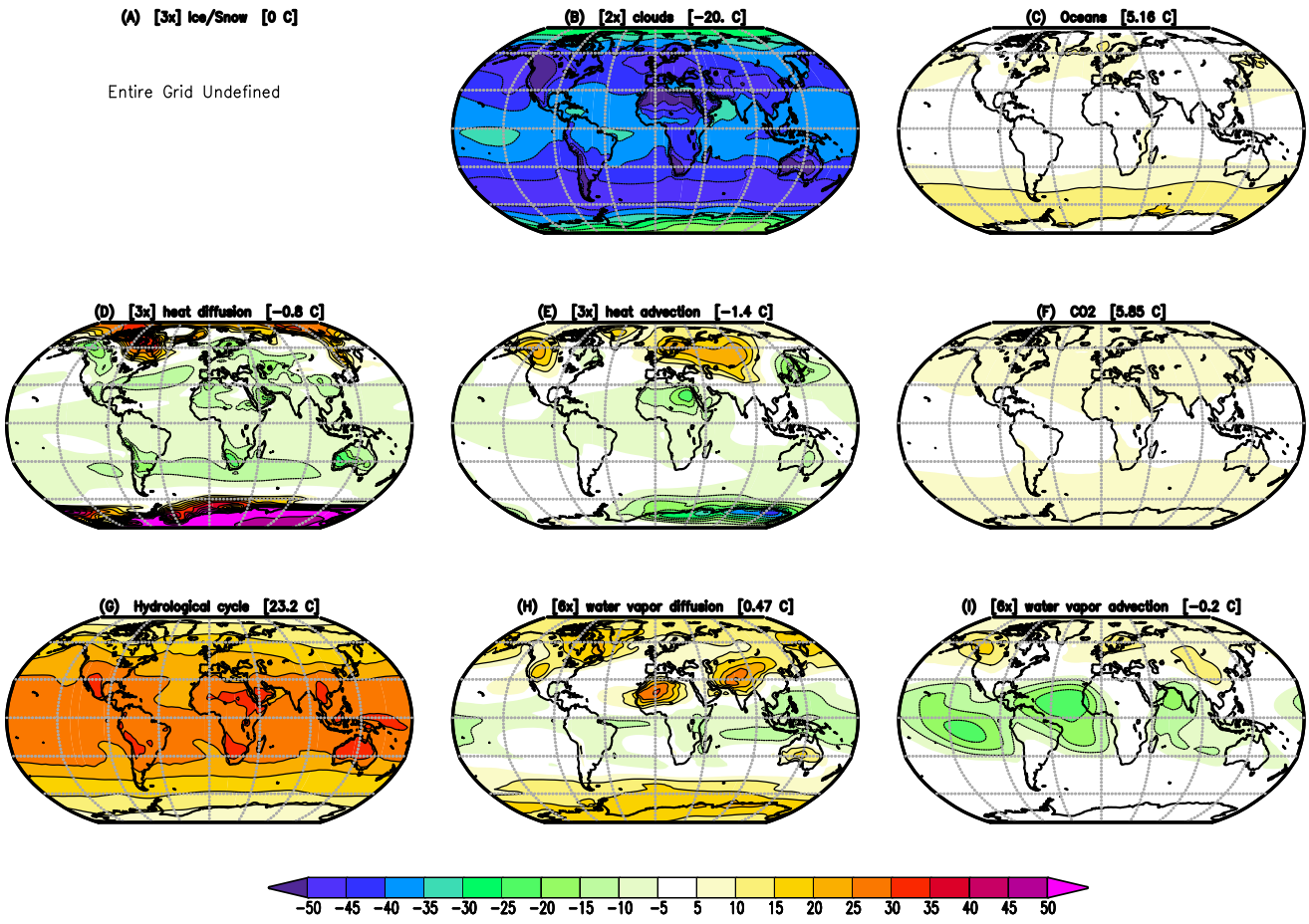

Supplementary Figure 2